UCSD/PTH 09-07

Chiral properties of $SU(3)$ sextet fermions

Zoltán Fodor [abcd], Kieran Holland [e], Julius Kuti [f],
Dániel Nógrádi [f] and Chris Schroeder [f]

[a] *Department of Theoretical Physics, University of Wuppertal Gaußstrasse 20, Wuppertal 42119, Germany*

[b] *NIC/DESY Zeuthen Forschungsgruppe Platanenalle 6, Zeuthen 15738, Germany*

[c] *Forschungszentrum Jülich, D-52425 Jülich, Germany*

[d] *Institute for Theoretical Physics, Eötvös University Pázmány Péter sétány 1/A, Budapest 1117, Hungary*

[e] *Department of Physics, University of the Pacific 6301 Pacific Avenue, Stockton, CA 95211, USA*

[f] *Department of Physics, University of California San Diego 9500 Gilman Dr, La Jolla, CA 92093, USA*

Emails
fodor@bodri.elte.hu, kholland@pacific.edu, jkuti@ucsd.edu
nogradi@bodri.elte.hu, crs@physics.ucsd.edu

Abstract

$SU(3)$ gauge theory with overlap fermions in the 2-index symmetric (sextet) and fundamental representations is considered. A priori it is not known what the pattern of chiral symmetry breaking is in a higher dimensional representation although the general expectation is that if two representations are both complex, the breaking pattern will be the same. This expectation is verified for the sextet at $N_f = 0$ in several exact zero mode sectors. It is shown that if the volume is large enough the same random matrix ensemble describes both the sextet and fundamental Dirac eigenvalues. The number of zero modes for the sextet increases approximately 5-fold relative to the fundamental in accordance with the index theorem for small lattice spacing but zero modes which do not correspond to integer topological charge do exist at larger lattice spacings. The zero mode number dependence of the random matrix model predictions correctly match the simulations in each sector and each representation.

1 Introduction

An elegant and attractive way of solving the hierarchy problem of the Standard Model is the technicolor paradigm [1, 2], for a review and additional references see [3]. The basic building block of any technicolor model is a non-abelian gauge theory coupled to some number of fermion flavors transforming in some representation of the gauge group. The renormalized coupling towards the infrared may run similarly to QCD, may exhibit a walking behavior or may run into a fixed point. Generically, it is possible to realize all three possibilities for a given gauge group by changing the representation and/or flavor number. If both the gauge group and the representation are fixed the flavor number will determine in which phase the gauge theory is in the infrared.

Chiral symmetry breaking is intimately tied to the infrared behavior. Clearly, if chiral symmetry is broken, the theory can not have a non-trivial conformal fixed point. At $N_f = 0$ chiral symmetry is broken and as N_f is increased at a critical N_f the theory will enter the conformal window. It is generally believed that the restoration of chiral symmetry will signal the lower edge of the conformal window. Strictly speaking this is not necessarily the case because in principle chiral symmetry can be intact while the theory is not conformal (for example by generating a dynamical scale not in the chiral condensate but another quantity) but the general expectation is that this exotic scenario will not take place.

In this work the 2-index symmetric (sextet) representation of $SU(3)$ is considered in the quenched approximation. This model with $N_f = 2$ fermions is attractive for phenomenology for several reasons. First, since the sextet is a complex representation, if chiral symmetry breaking does take place it is expected on general grounds to give rise to 3 Goldstone modes which will be eaten appropriately by the W and Z bosons. Second, the $N_f = 2$ value might not be far from the lower edge of the conformal window and the coupling might exhibit the necessary walking behavior. Third, the perturbative S-parameter is rather small making it plausible that the model can be made consistent with electro-weak precision data. The likely smallness of the S-parameter is a consequence of the fact that the fermion content is increased by increasing the dimension of the representation and not the flavor number [4, 5]. All of the above, of course, is only possible if the theory is below the conformal window. If chiral symmetry breaking does take place, this is clearly the case. This is our primary motivation for the current study of chiral properties of sextet fermions.

Overlap fermions [6] preserve chiral symmetry exactly and possess exact zero modes at finite lattice spacing. The zero modes are indicative of the topology of the underlying gauge field while near-zero modes give rise to chiral symmetry breaking via the Banks-Casher relation [7]. In the ε-regime random matrix theory (RMT) [8–11] gives detailed predictions for the statistical properties of non-zero modes. How well RMT actually describes the non-zero modes of the sextet overlap operator will be addressed in this work at $N_f = 0$. Our findings for the zero-modes and the associated questions about topology have been reported in [12].

A priori it is not known what the pattern of chiral symmetry breaking is in an arbitrary representation. On general grounds one expects the sextet breaking to be the same as for the fundamental representation because both representations are complex. This expectation is verified here by the observation that the same RMT ensemble, the chiral unitary one, describes both the fundamental and the sextet eigenvalues in each exact zero mode sector ν. The number of zero modes depends on the representation and once a gauge configuration is given the number of sextet zero modes is approximately 5 times the number of fundamental zero modes as dictated by the index theorem. The deviation from this rule is a lattice artifact which becomes less and less for decreasing lattice spacing [12]. The RMT predictions are sensitive to ν and the matching of the simulation to RMT with the correct number of ν is a highly non-trivial test. A staggered fermion study necessarily limited to the trivial sector has been reported in [13] and an overlap

study with two different $SU(2)$ representations and the fundamental of $SU(3)$ appeared in [].

Previous lattice studies with unusual fermion content include gauge groups $SU(2)$ and $SU(3)$ and various representations [12, 13, 15–42] which were largely motivated by the same considerations as mentioned here, with some exceptions.

2 Dirac spectrum

The low lying Dirac spectrum is indicative of the infrared properties of the theory. It will exhibit markedly different behavior if chiral symmetry is spontaneously broken or if the infrared dynamics is conformal. Using the Dirac spectrum as a tool to decide in which phase a gauge theory is has been suggested first in [29] and later this idea was applied in [39].

2.1 Chiral symmetry breaking and RMT

The Banks-Casher relation in a theory with spontaneous symmetry breaking relates the low end of the spectral Dirac density to the chiral condensate,

$$\Sigma = \lim_{m\to 0}\lim_{V\to\infty} \frac{\pi\rho(0)}{V} \,. \tag{1}$$

It also implies that the low-lying eigenvalues are dense in the sense that the average spacing is inversely proportional to the volume,

$$\langle \Delta\lambda \rangle = \frac{\pi}{\Sigma V} \,. \tag{2}$$

The low energy dynamics in a finite box of spatial extent L is accurately described by chiral perturbation theory if $f_\pi L \gg 1$. If in addition the quark mass is chosen such that $m_\pi L \ll 1$ the derivative terms in the chiral Lagrangian can be dropped. This ε-regime is then analytically calculable in the microscopic limit with the help of RMT which can also be directly derived from the chiral Lagrangian [44]. The comparison is valid in the microscopic large L limit, meaning that the Dirac eigenvalues λ and fermion masses m are rescaled, $\zeta = \lambda\Sigma V$ and $\mu = m\Sigma V$, where ζ and μ are kept finite. Hence the comparison is relevant for the small eigenvalues which are $\lambda \sim 1/V$.

The RMT description only depends on the rescaled fermion masses, N_f, the number of zero modes ν and the pattern of symmetry breaking. Since both the fundamental and sextet representations are complex, the symmetry breaking pattern is expected to be the same [43]. Then the relevant random matrix model is governed by the following partition function,

$$Z = \int dW dW^\dagger \det{}^{N_f}(D+m) \exp(-N \mathrm{tr}\, WW^\dagger) \,, \tag{3}$$

where the complex matrix W is $N \times (N+\nu)$ and the Dirac operator is,

$$D = \begin{pmatrix} 0 & iW \\ iW^\dagger & 0 \end{pmatrix} , \tag{4}$$

assuming degenerate fermion masses m. In the microscopic large N limit the mass m and eigenvalues λ are rescaled by N, $\zeta = 2N\lambda$, $\mu = 2Nm$, similarly to the gauge theory case and then $N \to \infty$. In this limit

the joint distribution of the k smallest eigenvalues, $\zeta_1 \leq \ldots \leq \zeta_k$, is given by [45–47]

$$\omega(\zeta_1,\ldots,\zeta_k) = \frac{1}{2}\zeta_k \exp(-\zeta_k^2/4) \prod_{i=1}^{k-1} \left(\zeta_i^{2\nu+1}(\zeta_i^2+\mu^2)^{N_f}\right) \prod_{i>j}^{k-1} (\zeta_i^2-\zeta_j^2)^2 \mu^{\nu N_f} \times \tag{5}$$

$$\frac{\mathcal{Z}_2(\sqrt{\mu^2+\zeta_k^2},\ldots,\sqrt{\mu^2+\zeta_k^2},\sqrt{\zeta_k^2-\zeta_1^2},\sqrt{\zeta_k^2-\zeta_1^2},\ldots\sqrt{\zeta_k^2-\zeta_{k-1}^2},\sqrt{\zeta_k^2-\zeta_{k-1}^2},\zeta_k,\ldots,\zeta_k)}{\mathcal{Z}_\nu(\mu,\ldots,\mu)} \tag{6}$$

where $\sqrt{\mu^2+\zeta_k^2}$ and ζ_k in the argument of $\mathcal{Z}_2$ appear N_f and ν times, respectively, while μ appears N_f times in the argument of $\mathcal{Z}_\nu$. The expression $\mathcal{Z}_a$ with any number of arguments is given by the ratio,

$$\mathcal{Z}_a(x_1,\ldots,x_m) = \frac{\det{}_{1\leq i,j\leq m}\left(x_j^{i-1} I_{a+i-1}(x_j)\right)}{\prod_{i>j}^m (x_i^2-x_j^2)}\,, \tag{7}$$

which has a finite limit if some of the x_i variables become degenerate. The distribution of the k^{th} eigenvalue is then,

$$p_k(\zeta_k) = \int_0^{\zeta_k} d\zeta_1 \int_{\zeta_1}^{\zeta_k} d\zeta_2 \ldots \int_{\zeta_{k-2}}^{\zeta_k} d\zeta_{k-1}\, \omega(\zeta_1,\ldots,\zeta_k)\,. \tag{8}$$

In order to match the gauge theory calculation onto the RMT prediction, the scale Σ needs to be determined so that the gauge theory eigenvalues can be rescaled appropriately by ΣV. In order to have a completely parameter free prediction we will consider the distribution of ratios of eigenvalues. The unknown scale Σ drops out from these at $N_f = 0$. For example the distribution of the ratio of the first and second eigenvalue, $r = \lambda_1/\lambda_2 = \zeta_1/\zeta_2 < 1$, is simply

$$p_{1,2}(r) = \int_0^\infty d\zeta_2\, \omega(r\zeta_2,\zeta_2)\,, \tag{9}$$

and can be directly compared with the corresponding distribution in the gauge theory. Similar integrals apply to any ratio $r = \lambda_j/\lambda_k$.

The universality of the RMT description is twofold. First, the spectral properties of the matrix model in the large N limit do not depend on the details of the matrix model potential, generic perturbations of the latter leave the former unchanged [48, 49]. In (3) we have chosen the simplest potential, a Gaussian. Second, the spectral properties of two different underlying theories is expected to match the same matrix model as long as N_f, rescaled fermion masses, number of zero modes and the pattern of chiral symmetry breaking is left intact. The pattern of chiral symmetry breaking is a priori unknown, although the general expectation [43] is that since both the sextet and the fundamental representations are complex for $SU(3)$ the pattern will be the same, $SU(N_f) \times SU(N_f)/SU(N_f)$. Hence it is expected that the same RMT ensemble, the chiral unitary, will describe both models.

The RMT predictions are different in each zero mode sector, labeled by ν. For the fundamental representation the index theorem equates ν with the topological charge but for higher dimensional representations the relation becomes $\nu = 2TQ$ where T is the trace normalization factor of the representation. Overlap fermions possess exact zero modes giving rise to a well-defined ν even at finite lattice spacing. However at finite lattice spacing $Q = \nu/2T$ can actually be a fractional number but the number of configurations with this property disappears in the continuum limit [12].

At realistic lattice spacing a sizable number of configurations have a non-integer $\nu/2T$ and the distribution of Dirac eigenvalues on these configurations can also be compared with RMT. This is possible because the RMT partition function is directly sensitive to the number of zero modes ν regardless of what its interpretation is in terms of topological charges in the underlying theory.

In the quenched approximation, $N_f = 0$, the condition $m_\pi L \ll 1$ is not relevant but the first condition, $f_\pi L \gg 1$, does impose a lower bound on L. How large L has to be in order to separate the rotator and Goldstone modes in the finite volume chiral Hamiltonian so that chiral perturbation theory is applicable, depends on the representation. We will see that different volumes will be required for the fundamental and sextet representations. However once the volume is large enough, the universal behavior sets in and the choice of representation will not matter anymore.

2.2 Conformal phase

If the theory flows to a non-trivial conformal fixed point in the infrared, no scale is generated and $\Sigma = 0$. The spectral density of the Dirac operator is

$$\rho(\lambda) \sim \lambda^{3-\gamma}\,, \tag{10}$$

where γ is the anomalous dimension of $\bar{\psi}\psi$ and is calculable in perturbation theory. Up to 2-loops the universal first two β-function coefficients determine the fixed point coupling g_* and $\gamma = O(g_*^2)$. This calculation can be trusted close to the upper end of the conformal window but might break down close to the lower end [50].

In the free case $g_* = 0$ and the eigenvalue spacing is inversely proportional to the linear size L in finite volume. The robust prediction of RMT in the chirally broken case was that the eigenvalue spacing is inversely proportional to the volume $V = L^4$; see (2). In the non-trivial conformal case $g_* > 0$ and what is expected to hold is that the eigenvalue spacing is inversely proportional to the linear size to some power which is much less than 4 but of course larger than 1. This is because anomalous dimensions can not deviate too much from the free value because the fixed point g_* can not deviate too much from 0 since chiral symmetry would be broken by a large coupling precluding the existence of a fixed point.

It is worth noting that the deconfined phase of QCD where chiral symmetry is restored, especially if the temperature is well above T_c, might bare some resemblance to theories with a weak-coupling conformal fixed point. The eigenvalue distribution also in this case does not follow RMT because chiral symmetry is intact. There exist models of the Dirac spectrum that match simulation data rather nicely [51, 52] and some ingredients of these models might very well prove useful for the study of weakly-coupled conformal gauge theories as well.

3 Simulations

The exact solution of the RMT model in the large N limit, given by (8, 9) for the eigenvalue distributions, is quite compact but still includes a number of integrals. The numerical evaluation of these integrals, especially for high ν and/or k, is not entirely straightforward due to large cancellations. Since in the sextet case $\nu = 5Q$ one encounters $\nu = 10, 15, \ldots$ quite frequently which are high enough so that the instabilities make the numerical integration cumbersome. We found it easier to directly simulate the matrix model (3).

3.1 RMT

In each zero mode sector, $0 \leq \nu \leq 15$, the random matrix model (3) at $N_f = 0$ was simulated for $N = 300, 400, 500$ and 600. The number of configurations was around $50,000$ for each and since their deviation from each other was negligible relative to the statistical uncertainty in the gauge theory simulation, $N = 600$ was chosen as the $N \to \infty$ limit. The RMT results quoted in the remainder of this work are based on $N = 600$ ensembles, with about $110,000$ configurations in each sector (except for low k and ν where the exact results are used in some of the plots).

The expectation values of the first 10 eigenvalues are listed in Table 3 for $0 \leq \nu \leq 15$.

3.2 Gauge theory

The eigenvalues of the overlap operator D lie on a circle of radius ρ/a centered at $(\rho/a, 0)$ where $-\rho/a$ is the negative Wilson mass entering its definition. The non-real eigenvalues come in pairs, $\lambda_1 \pm i\lambda_2$, with $\lambda_{1,2} > 0$. Picking the ones on the upper half plane, these are then stereographically projected from $(2\rho/a, 0)$ onto the positive imaginary axis to obtain the real and positive eigenvalues λ that are used for the comparison with RMT,

$$\lambda = \frac{\lambda_2}{1 - \frac{a\lambda_1}{2\rho}} \ . \tag{11}$$

For the sextet representation, $2T = 5$. This means that about 5 times more eigenvalues have to be computed for the sextet operator than for the fundamental in order to end up with non-zero eigenvalues. The dimension of the sextet representation is 2 times larger than the fundamental resulting in 4 times more operations. These two facts result in about an order of magnitude increase in computational cost for sextet eigenvalues relative to the fundamental. A comparison of RMT and QCD with overlap fundamental fermions has been reported in [53] for $N_f = 0$ and in [54] for $N_f = 2$. The sextet representation and RMT have been considered in [13] within the staggered formulation.

The simulation parameters are summarized in Table 1. The lattices in set A have physical volume $L = 1.2215\, fm$ and the lattices in set B have $L = 1.4658\, fm$. There are 5 and 2 lattice spacings in the two sets. The scale is set by the static fundamental representation quark potential through $r_0 = 0.5\, fm$ [55]. The negative Wilson mass in the overlap operator was set to -1.40 for the fundamental and -1.70 for the sextet representation. Two steps of stout smearing was applied with smearing parameter 0.15 for both representations [56]. The implementation of the overlap operator is the same as in [57] and the gauge action is the Wilson plaquette.

3.3 Parameter free comparisons with RMT

First let us compare the eigenvalue ratios $\langle\lambda_i\rangle/\langle\lambda_j\rangle$ with the RMT predictions. These do not require the fitting of any parameter, these are completely parameter free predictions in each zero mode sector. Figure 1 shows these ratios for both representations for the A lattices and $i, j = 1, 2, 3, 4$ in the $\nu = 0$ sector.

Already from the $\nu = 0$ sector it is clear that the measured eigenvalue ratios are consistently below the RMT predictions for the fundamental representation for most of the points, i.e. the fixed $L = 1.2215\, fm$ volume is too small. This same volume is large enough for the sextet representation though, and the measured ratios fit the RMT predictions very nicely.

The observation that a given volume can be too small for the fundamental but large enough for the sextet representation is not entirely a surprise. In [16] it was noted long ago that the critical coupling

	β	L/a	r_0/a	$a\,[fm]$	#config
A_1	5.9500	12	4.9122	0.1018	441
A_2	6.0384	14	5.7306	0.0873	543
A_3	6.1210	16	6.5496	0.0763	408
A_4	6.2719	20	8.1866	0.0611	211
A_5	6.4064	24	9.8239	0.0509	105
B_1	6.0096	16	5.4574	0.0916	351
B_2	6.1474	20	6.8225	0.0733	228

Table 1: Simulation parameters for the Wilson plaquette gauge action. The physical volume is kept fixed in each set A and B, $L/r_0 = 2.4429$ and 2.9315, respectively, corresponding to $L = 1.2215\,fm$ and $1.4658\,fm$, respectively.

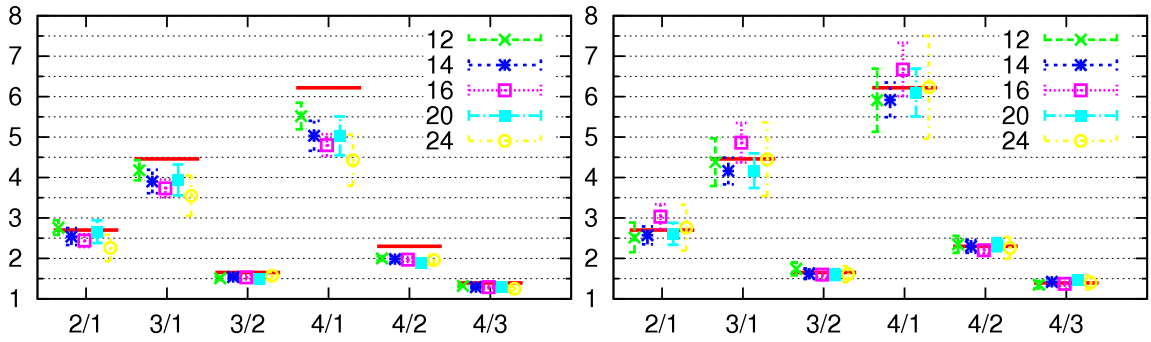

Figure 1: Ratios of measured average eigenvalues $\langle\lambda_i\rangle/\langle\lambda_j\rangle$ for the fundamental (left) and sextet (right) representations on the A lattices, $L = 1.2215\,fm$, in the $\nu = 0$ sector for all five L/a values. The RMT predictions (horizontal lines) are the same for both.

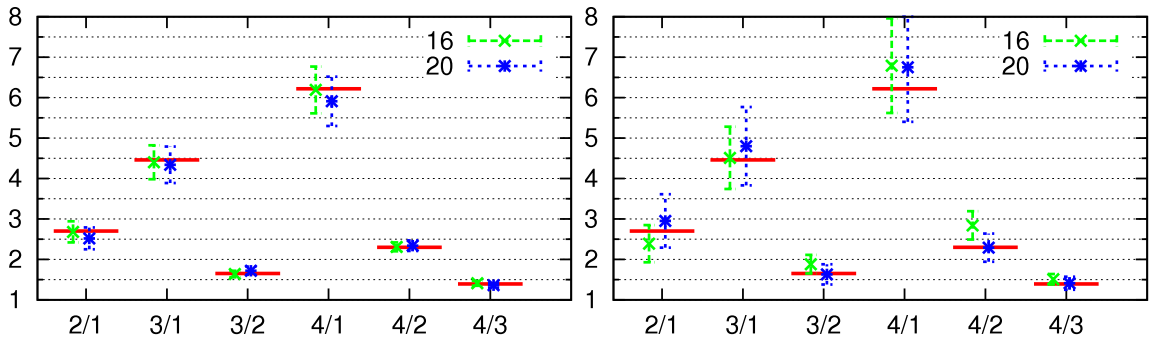

Figure 2: Ratios of measured average eigenvalues $\langle\lambda_i\rangle/\langle\lambda_j\rangle$ for the fundamental (left) and sextet (right) representations on the B lattices, $L = 1.4658\,fm$, in the $\nu = 0$ sector for the two L/a values. The RMT predictions (horizontal lines) are the same for both.

of chiral symmetry breaking β_c for the sextet is much larger than for the fundamental in the quenched approximation. This means that as long as β is chosen the same and below β_c for both theories, the sextet model will be deeper in its chirally broken phase than the fundamental model.

The eigenvalue ratios are shown on Figure 2 for the B lattices where the volume is larger. This volume is apparently large enough so that both theories enter the ε-regime and the RMT predictions work for both representations. Since the pattern of symmetry breaking for the two representations is expected to be the same it is expected that the same universal RMT describes the low-lying Dirac eigenvalues. Figure 2 confirms this universal property of RMT, the two underlying theories are clearly different, but in the microscopic limit where RMT is expected to hold, they display the same universal behavior.

Tables 4 - 19 list the eigenvalue ratios for all sectors $0 \leq \nu \leq 15$, both lattices A and B and both representations (except for lattices A and the fundamental where we have seen from the $\nu = 0$ sector that the volume is too small). These tables are sparse for several reasons. One is that if the maximal fundamental index in an ensemble is ν, then the maximal sextet index will be roughly 5ν and there will be no fundamental index between ν and 5ν. Also, since the sextet index tends to come in 5-tuples for small lattice spacing, indices which are not a multiple of 5 will have small or no statistics. In addition, we calculate a fixed number of eigenvalues and it can happen that the number of computed eigenvalues is only 1, 2, 3, etc. more than the number of zero modes. In this case λ_k for larger k will not be available.

The eigenvalue ratios in the Tables 4 - 19 are mostly within one standard deviation from the RMT predictions. More precisely, this happens for 65% and 81% of the cases for the sextet on the B_1 and B_2 lattices, 72% and 53% for the fundamental on the B_1 and B_2 lattices and $76\%, 86\%, 87\%, 87\%$ and 94% of the cases on the $A_1, \ldots, A_5$ lattices for the sextet. If the comparison is only made for the first 5 eigenvalues then the results are within one standard deviation from the RMT predictions for $83\%, 91\%, 71\%, 78\%, 80\%, 85\%, 85\%, 87\%$ and 94% of the cases, in the same order as above. This we take as confirmation that the RMT predictions about the statistical properties of small Dirac eigenvalues are correct.

Not only the averages but also the entire distribution of eigenvalue ratios can be compared with the RMT predictions. Figures 3 - 7 show the sextet eigenvalue ratio distributions in various zero mode sectors on the A lattices. Figures 8 and 9 show the same for the larger B lattices for the sextet, while fundamental eigenvalue ratio distributions are on Figures 10 and 11.

	A_1	A_2	A_3	A_4	A_5	B_1	B_2
a/r_0	0.2036	0.1745	0.1527	0.1222	0.1018	0.1832	0.1466
$r_0^3\Sigma_F$						0.37(6)	0.35(3)
$r_0^3\Sigma_S$	2.0(2)	2.2(1)	2.5(3)	2.5(2)	2.6(5)	2.9(5)	2.9(3)

Table 2: The chiral condensate Σ from the average first eigenvalue in the $\nu = 0$ sector for the two representations. The volume of the A lattices is too small for the fundamental representation and Σ is not determined in this case.

The displayed errors on the histograms are jackknife errors. The level of agreement with the RMT predictions may be characterized by the χ^2/dof value of the simulation results and the RMT curves using the jackknife errors on each bin. These χ^2/dof values are displayed on each plot, they are all close to 1. The smallest is 0.11 and the largest is 3.23; for more details see the top right corner of each plot.

Clearly, the same quenched lattices induce the correct ν-dependent distributions for the eigenvalue ratios depending on the representation. The roughly 5-fold increase in ν for the sextet relative to the fundamental is correctly captured by the ν-dependent distribution of non-zero modes. These agreements are very non-trivial checks of the statement that the pattern of chiral symmetry breaking is the same for the sextet as for the fundamental.

3.4 Scale matching

The only unknown parameter needed for a general comparison of simulations with RMT is the rescaling factor Σ, which in the quenched theory is only thought of as a low energy constant without a real physical meaning in terms of fermion bilinears. In the previous section ratios of eigenvalues were considered from which Σ drops out. In this section Σ will be determined from the average smallest eigenvalue in the $\nu = 0$ sector and the predictions of RMT for eigenvalue distributions in all sectors will be compared with the simulations.

This means that Σ is determined from the relation,

$$\langle \zeta_1 \rangle_0 = \langle \lambda_1 \rangle_0 \Sigma V \ , \tag{12}$$

where the left hand side is evaluated from RMT and the right hand side is the result of the simulation. Since we have seen that for the fundamental representation the A lattices are too small, the comparison will not be done in this case. The resulting values of Σ are shown in Table 2. As long as a not too high k is chosen, a different determination of Σ from the k^{th} eigenvalue in other zero mode sectors gives compatible values.

Using the numerically determined chiral condensate the distributions of the eigenvalues can be compared with the RMT predictions. The level of agreement is very similar to the case of the eigenvalue ratios.

The non-trivial ν-dependent matching – similarly to the parameter-free agreement of the previous section – between the gauge theory simulation in the sextet representation and the chiral unitary RMT is showing that the pattern of chiral symmetry breaking is the same as for the fundamental representation. It also suggests that if chiral symmetry breaking does take place with $N_f = 2$ sextet fermions then the pattern will also be the same as with $N_f = 2$ fundamental fermions. If this happens to be the case then the number of Goldstone bosons will be 3, as expected on general grounds, which would be the appropriate

number for phenomenological applications in technicolor models. It should be noted that some, although non-conclusive, data has been presented in [24,39] which appear to indicate that the $N_f = 2$ model might already be conformal.

4 Conclusion

We have shown that if the physical volume is large enough and the system enters into the ε-regime the predictions of the same random matrix theory are accurately describing $SU(3)$ gauge theory with fermions in both the fundamental and sextet representations at $N_f = 0$ and various zero mode sectors. Since the number of zero modes depends on the representation and the matching with RMT is correct in this non-trivial ν-dependent manner we take this as further evidence that the pattern of chiral symmetry breaking is the same for the sextet and the fundamental, complementing earlier results with staggered fermions in the trivial sector [13].

An important aspect of the calculation was the use of overlap fermions which possess exact zero modes. In addition, it is expected that for all gauge groups and all representations the universality class is correctly singled out by overlap fermions, a property that is not present in the staggered formulation for certain real representations. These representations may turn out to play an important role in technicolor models.

The application in technicolor models was our primary motivation. The topological and chiral properties of overlap fermions in higher dimensional representations can help in identifying in which phase a non-abelian gauge theory is in the infrared, whether chiral symmetry breaking does take place or the dynamics is conformal. After the present quenched study we plan to extend these methods to dynamical simulations where the potentially strong coupling can make the perturbative predictions regarding a conformal fixed point unreliable.

Acknowledgments

DN would like to acknowledge useful correspondence with Urs Heller. The computations were carried out on the USQCD clusters at Fermilab and GPU clusters at Wuppertal University [58]. This work is supported by the NSF under grant 0704171, by the DOE under grants DOE-FG03-97ER40546, DOE-FG-02-97ER25308, by the DFG under grant FO 502/1 and by SFB-TR/55.

References

[1] S. Weinberg, Phys. Rev. D **13** (1976) 974.

[2] L. Susskind, Phys. Rev. D **20**, 2619 (1979).

[3] C. T. Hill and E. H. Simmons, Phys. Rept. **381**, 235 (2003) [Erratum-ibid. **390**, 553 (2004)] [arXiv:hep-ph/0203079].

[4] F. Sannino and K. Tuominen, Phys. Rev. D **71**, 051901 (2005) [arXiv:hep-ph/0405209].

[5] D. D. Dietrich and F. Sannino, Phys. Rev. D **75**, 085018 (2007) [arXiv:hep-ph/0611341].

[6] H. Neuberger, Phys. Lett. B **417** (1998) 141 [arXiv:hep-lat/9707022].

[7] T. Banks and A. Casher, Nucl. Phys. B **169**, 103 (1980).

[8] E. V. Shuryak and J. J. M. Verbaarschot, Nucl. Phys. A **560**, 306 (1993) [arXiv:hep-th/9212088].

[9] J. J. M. Verbaarschot and I. Zahed, Phys. Rev. Lett. **70**, 3852 (1993) [arXiv:hep-th/9303012].

[10] J. J. M. Verbaarschot, Phys. Rev. Lett. **72**, 2531 (1994) [arXiv:hep-th/9401059].

[11] A. M. Halasz and J. J. M. Verbaarschot, Phys. Rev. D **52**, 2563 (1995) [arXiv:hep-th/9502096].

[12] Z. Fodor, K. Holland, J. Kuti, D. Nogradi and C. Schroeder, arXiv:0905.3586 [hep-lat].

[13] P. H. Damgaard, U. M. Heller, R. Niclasen and B. Svetitsky, Nucl. Phys. B **633**, 97 (2002) [arXiv:hep-lat/0110028].

[14] R. G. Edwards, U. M. Heller, J. E. Kiskis and R. Narayanan, Phys. Rev. Lett. **82**, 4188 (1999) [arXiv:hep-th/9902117].

[15] J. B. Kogut, M. Stone, H. W. Wyld, J. Shigemitsu, S. H. Shenker and D. K. Sinclair, Phys. Rev. Lett. **48**, 1140 (1982).

[16] J. B. Kogut, J. Shigemitsu and D. K. Sinclair, Phys. Lett. B **145**, 239 (1984).

[17] Y. Iwasaki, K. Kanaya, S. Sakai and T. Yoshie, Phys. Rev. Lett. **69**, 21 (1992).

[18] P. H. Damgaard, U. M. Heller, A. Krasnitz and P. Olesen, Phys. Lett. B **400**, 169 (1997) [arXiv:hep-lat/9701008].

[19] F. Karsch and M. Lutgemeier, Nucl. Phys. B **550**, 449 (1999) [arXiv:hep-lat/9812023].

[20] Y. Iwasaki, K. Kanaya, S. Kaya, S. Sakai and T. Yoshie, Phys. Rev. D **69**, 014507 (2004) [arXiv:hep-lat/0309159].

[21] S. Catterall and F. Sannino, Phys. Rev. D **76**, 034504 (2007) [arXiv:0705.1664 [hep-lat]].

[22] T. Appelquist, G. T. Fleming and E. T. Neil, Phys. Rev. Lett. **100**, 171607 (2008) [arXiv:0712.0609 [hep-ph]].

[23] T. DeGrand, Y. Shamir and B. Svetitsky, Phys. Rev. D **79**, 034501 (2009) [arXiv:0812.1427 [hep-lat]].

[24] Y. Shamir, B. Svetitsky and T. DeGrand, Phys. Rev. D **78**, 031502 (2008) [arXiv:0803.1707 [hep-lat]].

[25] L. Del Debbio, A. Patella and C. Pica, arXiv:0812.0570 [hep-lat].

[26] L. Del Debbio, A. Patella and C. Pica, arXiv:0805.2058 [hep-lat].

[27] L. Del Debbio, B. Lucini, A. Patella, C. Pica and A. Rago, arXiv:0907.3896 [hep-lat].

[28] Z. Fodor, K. Holland, J. Kuti, D. Nogradi and C. Schroeder, arXiv:0809.4890 [hep-lat].

[29] Z. Fodor, K. Holland, J. Kuti, D. Nogradi and C. Schroeder, arXiv:0809.4888 [hep-lat].

[30] S. Catterall, J. Giedt, F. Sannino and J. Schneible, JHEP **0811**, 009 (2008) [arXiv:0807.0792 [hep-lat]].

[31] A. J. Hietanen, J. Rantaharju, K. Rummukainen and K. Tuominen, JHEP **0905**, 025 (2009) [arXiv:0812.1467 [hep-lat]].

[32] A. Deuzeman, M. P. Lombardo and E. Pallante, Phys. Lett. B **670**, 41 (2008) [arXiv:0804.2905 [hep-lat]].

[33] A. Armoni, B. Lucini, A. Patella and C. Pica, Phys. Rev. D **78**, 045019 (2008) [arXiv:0804.4501 [hep-th]].

[34] X. Y. Jin and R. D. Mawhinney, PoS **LATTICE2008**, 059 (2008) [arXiv:0812.0413 [hep-lat]].

[35] T. Appelquist, G. T. Fleming and E. T. Neil, arXiv:0901.3766 [hep-ph].

[36] A. J. Hietanen, K. Rummukainen and K. Tuominen, arXiv:0904.0864 [hep-lat].

[37] A. Hietanen, J. Rantaharju, K. Rummukainen and K. Tuominen, Nucl. Phys. A **820** (2009) 191C.

[38] A. Deuzeman, M. P. Lombardo and E. Pallante, arXiv:0904.4662 [hep-ph].

[39] T. DeGrand, arXiv:0906.4543 [hep-lat].

[40] A. Hasenfratz, arXiv:0907.0919 [hep-lat].

[41] Z. Fodor, K. Holland, J. Kuti, D. Nogradi and C. Schroeder, arXiv:0907.4562 [hep-lat].

[42] K. i. Nagai, G. Carrillo-Ruiz, G. Koleva and R. Lewis, arXiv:0908.0166 [hep-lat].

[43] S. Dimopoulos, Nucl. Phys. B **168**, 69 (1980).

[44] J. C. Osborn, D. Toublan and J. J. M. Verbaarschot, Nucl. Phys. B **540**, 317 (1999) [arXiv:hep-th/9806110].

[45] T. Nagao and S. M. Nishigaki, Phys. Rev. D **62**, 065006 (2000) [arXiv:hep-th/0001137].

[46] P. H. Damgaard and S. M. Nishigaki, Phys. Rev. D **63**, 045012 (2001) [arXiv:hep-th/0006111].

[47] P. H. Damgaard, U. M. Heller, R. Niclasen and K. Rummukainen, Phys. Lett. B **495**, 263 (2000) [arXiv:hep-lat/0007041].

[48] G. Akemann, P. H. Damgaard, U. Magnea and S. Nishigaki, Nucl. Phys. B **487**, 721 (1997) [arXiv:hep-th/9609174].

[49] P. H. Damgaard and S. M. Nishigaki, Nucl. Phys. B **518**, 495 (1998) [arXiv:hep-th/9711023].

[50] T. Banks and A. Zaks, Nucl. Phys. B **196**, 189 (1982).

[51] T. G. Kovacs, PoS **LATTICE2008**, 198 (2008) [arXiv:0810.4763 [hep-lat]].

[52] T. G. Kovacs, arXiv:0906.5373 [hep-lat].

[53] L. Giusti, M. Luscher, P. Weisz and H. Wittig, JHEP **0311**, 023 (2003) [arXiv:hep-lat/0309189].

[54] H. Fukaya *et al.*, Phys. Rev. D **76**, 054503 (2007) [arXiv:0705.3322 [hep-lat]].

[55] S. Necco and R. Sommer, Nucl. Phys. B **622**, 328 (2002) [arXiv:hep-lat/0108008].

[56] C. Morningstar and M. J. Peardon, Phys. Rev. D **69**, 054501 (2004) [arXiv:hep-lat/0311018].

[57] Z. Fodor, S. D. Katz and K. K. Szabo, JHEP **0408**, 003 (2004) [arXiv:hep-lat/0311010].

[58] G. I. Egri, Z. Fodor, C. Hoelbling, S. D. Katz, D. Nogradi and K. K. Szabo, Comput. Phys. Commun. **177**, 631 (2007) [arXiv:hep-lat/0611022].

ν	k	$\langle\zeta_k\rangle_\nu$	ν	k	$\langle\zeta_k\rangle_\nu$	ν	k	$\langle\zeta_k\rangle_\nu$	ν	k	$\langle\zeta_k\rangle_\nu$
0	1	1.777(6)	4	1	6.68(2)	8	1	11.15(3)	12	1	15.47(5)
0	2	4.79(1)	4	2	10.23(3)	8	2	15.09(4)	12	2	19.73(6)
0	3	7.90(2)	4	3	13.55(4)	8	3	18.64(6)	12	3	23.48(7)
0	4	11.03(3)	4	4	16.80(5)	8	4	22.04(7)	12	4	27.02(8)
0	5	14.16(4)	4	5	20.00(6)	8	5	25.36(8)	12	5	30.46(9)
0	6	17.30(5)	4	6	23.19(7)	8	6	28.64(8)	12	6	33.83(10)
0	7	20.44(6)	4	7	26.37(8)	8	7	31.89(9)	12	7	37.14(11)
0	8	23.57(7)	4	8	29.55(9)	8	8	35.11(10)	12	8	40.44(12)
0	9	26.71(8)	4	9	32.70(10)	8	9	38.32(11)	12	9	43.70(13)
0	10	29.85(9)	4	10	35.86(11)	8	10	41.52(12)	12	10	46.93(14)
1	1	3.11(1)	5	1	7.83(2)	9	1	12.24(4)	13	1	16.53(5)
1	2	6.26(2)	5	2	11.47(3)	9	2	16.26(5)	13	2	20.86(6)
1	3	9.42(3)	5	3	14.86(4)	9	3	19.87(6)	13	3	24.66(7)
1	4	12.56(4)	5	4	18.14(5)	9	4	23.31(7)	13	4	28.24(8)
1	5	15.69(5)	5	5	21.38(6)	9	5	26.67(8)	13	5	31.71(10)
1	6	18.83(6)	5	6	24.59(7)	9	6	29.97(9)	13	6	35.09(11)
1	7	21.98(6)	5	7	27.78(8)	9	7	33.23(10)	13	7	38.43(12)
1	8	25.12(7)	5	8	30.96(9)	9	8	36.47(11)	13	8	41.73(13)
1	9	28.26(8)	5	9	34.13(10)	9	9	39.69(12)	13	9	45.01(13)
1	10	31.41(9)	5	10	37.29(11)	9	10	42.89(13)	13	10	48.26(14)
2	1	4.34(1)	6	1	8.94(3)	10	1	13.32(4)	14	1	17.60(5)
2	2	7.64(2)	6	2	12.69(4)	10	2	17.42(5)	14	2	22.00(7)
2	3	10.84(3)	6	3	16.14(5)	10	3	21.08(6)	14	3	25.84(8)
2	4	14.01(4)	6	4	19.46(6)	10	4	24.56(7)	14	4	29.45(9)
2	5	17.17(5)	6	5	22.73(7)	10	5	27.95(8)	14	5	32.95(10)
2	6	20.33(6)	6	6	25.97(8)	10	6	31.26(9)	14	6	36.36(11)
2	7	23.48(7)	6	7	29.17(9)	10	7	34.54(10)	14	7	39.72(12)
2	8	26.62(8)	6	8	32.36(10)	10	8	37.79(11)	14	8	43.03(13)
2	9	29.77(9)	6	9	35.55(11)	10	9	41.03(12)	14	9	46.33(14)
2	10	32.92(10)	6	10	38.73(12)	10	10	44.25(13)	14	10	49.59(15)
3	1	5.53(2)	7	1	10.04(3)	11	1	14.39(4)	15	1	18.65(6)
3	2	8.95(3)	7	2	13.90(4)	11	2	18.59(6)	15	2	23.13(7)
3	3	12.22(4)	7	3	17.39(5)	11	3	22.28(7)	15	3	27.01(8)
3	4	15.42(5)	7	4	20.75(6)	11	4	25.80(8)	15	4	30.66(9)
3	5	18.61(6)	7	5	24.05(7)	11	5	29.20(9)	15	5	34.18(10)
3	6	21.78(6)	7	6	27.31(8)	11	6	32.55(10)	15	6	37.61(11)
3	7	24.93(7)	7	7	30.54(9)	11	7	35.85(11)	15	7	40.98(12)
3	8	28.09(8)	7	8	33.74(10)	11	8	39.12(12)	15	8	44.32(13)
3	9	31.24(9)	7	9	36.94(11)	11	9	42.37(13)	15	9	47.62(14)
3	10	34.39(10)	7	10	40.12(12)	11	10	45.60(14)	15	10	50.89(15)

Table 3: RMT expectation values of the first 10 eigenvalues in each sector ν.

j/k	RMT	$B_1(S)$	$B_2(S)$	$B_1(F)$	$B_2(F)$	$A_1(S)$	$A_2(S)$	$A_3(S)$	$A_4(S)$	$A_5(S)$
2/1	2.703	2.39(46)	2.95(66)	2.68(26)	2.52(27)	2.52(37)	2.57(22)	3.03(31)	2.61(27)	2.76(57)
3/1	4.460	4.51(77)	4.80(97)	4.40(42)	4.34(45)	4.38(59)	4.16(33)	4.86(49)	4.17(43)	4.45(91)
4/1	6.220	6.8(1.2)	6.8(1.4)	6.19(58)	5.91(61)	5.91(78)	5.92(43)	6.67(66)	6.10(59)	6.2(1.3)
5/1	7.991	8.7(1.5)	8.1(1.6)	7.99(75)	7.30(74)	7.12(94)	7.87(71)	8.66(86)	7.73(72)	8.2(1.6)
6/1	9.759	10.4(1.8)	10.1(1.9)	9.49(87)	8.69(87)	8.8(1.2)	9.45(88)	10.6(1.0)	9.55(89)	10.0(1.9)
7/1	11.532	12.6(2.1)	12.0(2.3)		9.54(99)		11.18(94)	13.0(1.3)	11.3(1.0)	11.4(2.2)
8/1	13.300	14.4(2.5)	14.3(2.7)				13.1(1.1)	14.9(1.6)	12.9(1.2)	13.1(2.5)
9/1	15.072	16.6(2.8)	16.1(3.1)				14.8(1.2)	17.0(1.8)	14.7(1.3)	14.7(2.8)
10/1	16.844	19.1(3.2)	18.5(3.5)				16.8(1.3)	18.8(2.0)		16.4(3.1)
3/2	1.650	1.88(23)	1.63(25)	1.64(8)	1.72(10)	1.74(16)	1.62(13)	1.60(7)	1.60(13)	1.61(20)
4/2	2.301	2.84(35)	2.29(35)	2.31(11)	2.34(13)	2.35(21)	2.30(16)	2.20(9)	2.34(16)	2.26(27)
5/2	2.956	3.62(44)	2.74(40)	2.98(14)	2.89(15)	2.82(26)	3.06(27)	2.86(11)	2.96(19)	2.99(32)
6/2	3.611	4.35(54)	3.43(48)	3.54(15)	3.45(16)	3.51(31)	3.67(34)	3.49(13)	3.66(24)	3.63(37)
7/2	4.266	5.25(64)	4.06(57)		3.78(21)		4.34(36)	4.29(21)	4.31(27)	4.15(43)
8/2	4.920	6.03(72)	4.84(68)				5.10(41)	4.93(27)	4.95(31)	4.75(48)
9/2	5.576	6.93(84)	5.44(78)				5.74(46)	5.61(30)	5.63(34)	5.31(51)
10/2	6.231	7.96(94)	6.26(88)				6.53(51)	6.20(32)		5.95(58)
4/3	1.395	1.51(13)	1.41(16)	1.41(6)	1.36(6)	1.35(9)	1.42(9)	1.37(5)	1.46(10)	1.40(17)
5/3	1.792	1.92(16)	1.68(18)	1.82(8)	1.68(7)	1.62(11)	1.89(16)	1.78(7)	1.85(12)	1.86(19)
6/3	2.188	2.31(21)	2.10(21)	2.16(8)	2.00(7)	2.02(14)	2.27(20)	2.18(8)	2.29(15)	2.25(23)
7/3	2.586	2.79(24)	2.49(25)		2.20(10)		2.69(21)	2.67(12)	2.70(17)	2.57(26)
8/3	2.982	3.20(27)	2.97(30)				3.15(24)	3.07(17)	3.10(19)	2.95(29)
9/3	3.379	3.68(31)	3.34(34)				3.55(26)	3.50(18)	3.53(21)	3.30(31)
10/3	3.777	4.22(34)	3.84(38)				4.04(29)	3.87(19)		3.69(35)
5/4	1.285	1.28(11)	1.20(12)	1.29(5)	1.24(5)	1.20(8)	1.33(10)	1.30(5)	1.27(7)	1.33(14)
6/4	1.569	1.53(14)	1.49(15)	1.53(5)	1.47(5)	1.50(9)	1.60(13)	1.59(6)	1.56(8)	1.61(16)
7/4	1.854	1.85(16)	1.77(17)		1.62(7)		1.89(13)	1.95(9)	1.84(9)	1.84(18)
8/4	2.138	2.12(18)	2.11(21)				2.22(15)	2.24(12)	2.12(10)	2.11(20)
9/4	2.423	2.44(21)	2.38(24)				2.50(17)	2.55(13)	2.41(11)	2.35(22)
10/4	2.708	2.80(22)	2.73(27)				2.84(18)	2.82(14)		2.64(24)
6/5	1.221	1.20(11)	1.25(11)	1.19(4)	1.19(3)	1.24(8)	1.20(12)	1.22(4)	1.24(6)	1.21(10)
7/5	1.443	1.45(12)	1.48(13)		1.31(5)		1.42(13)	1.50(7)	1.46(6)	1.39(11)
8/5	1.664	1.67(14)	1.77(15)				1.67(15)	1.72(9)	1.67(7)	1.59(13)
9/5	1.886	1.91(16)	1.99(18)				1.88(16)	1.96(10)	1.90(8)	1.77(13)
10/5	2.108	2.20(17)	2.29(20)				2.14(18)	2.17(10)		1.99(15)
7/6	1.182	1.21(11)	1.19(9)		1.10(4)		1.18(11)	1.23(5)	1.18(5)	1.14(9)
8/6	1.363	1.38(12)	1.41(11)				1.39(12)	1.41(7)	1.35(6)	1.31(10)
9/6	1.544	1.59(14)	1.59(13)				1.56(14)	1.61(8)	1.54(6)	1.46(10)
10/6	1.726	1.83(15)	1.83(15)				1.78(15)	1.78(8)		1.64(11)
8/7	1.153	1.15(9)	1.19(9)				1.17(9)	1.15(7)	1.15(4)	1.15(9)
9/7	1.307	1.32(11)	1.34(11)				1.32(10)	1.31(7)	1.30(5)	1.28(9)
10/7	1.461	1.52(12)	1.54(12)				1.50(12)	1.45(8)		1.43(10)
9/8	1.133	1.15(9)	1.13(9)				1.12(9)	1.14(7)	1.14(4)	1.12(7)
10/8	1.266	1.32(10)	1.29(10)				1.28(10)	1.26(8)		1.25(8)
10/9	1.118	1.15(9)	1.15(9)				1.14(8)	1.11(7)		1.12(7)

Table 4: Average eigenvalue ratios in the $\nu = 0$ sector in RMT and the A_i and B_i lattices.

j/k	RMT	$B_1(S)$	$B_2(S)$	$B_1(F)$	$B_2(F)$	$A_1(S)$	$A_2(S)$	$A_3(S)$	$A_4(S)$	$A_5(S)$
2/1	2.016	1.95(20)	1.64(23)	2.20(9)	2.10(10)	2.01(14)	2.09(24)	2.07(34)	2.08(52)	
3/1	3.031	2.87(28)	2.54(38)	3.37(13)	3.15(16)	3.05(24)	3.00(32)	3.18(51)	3.35(78)	
4/1	4.041	3.79(39)	3.22(44)	4.63(17)	4.18(19)	3.97(35)	4.13(56)	4.30(68)	4.9(1.1)	
5/1	5.050	4.80(52)	4.21(58)	5.67(21)	5.12(23)	5.07(46)	5.41(75)	5.46(87)	6.5(1.5)	
6/1	6.060	5.73(59)	5.23(72)	6.55(24)	5.95(26)	6.02(53)	6.51(89)	6.9(1.1)	8.2(1.9)	
7/1	7.073	6.79(70)	6.02(83)	7.5(1.1)	6.59(29)		7.38(97)	8.2(1.3)	9.4(2.2)	
8/1	8.082	8.14(86)	6.96(97)				8.7(1.1)	9.5(1.4)	10.7(2.5)	
9/1	9.093	9.43(99)	8.0(1.1)				9.5(1.2)	10.7(1.7)		
10/1	10.106	10.7(1.1)	9.1(1.3)				10.7(1.2)	11.9(1.9)		
3/2	1.504	1.47(9)	1.55(17)	1.53(4)	1.50(6)	1.51(10)	1.43(14)	1.54(18)	1.61(22)	
4/2	2.005	1.94(13)	1.96(19)	2.10(5)	1.99(6)	1.97(15)	1.97(25)	2.08(24)	2.34(29)	
5/2	2.505	2.46(19)	2.57(26)	2.57(7)	2.44(7)	2.52(20)	2.58(33)	2.64(31)	3.11(39)	
6/2	3.007	2.94(21)	3.19(31)	2.97(7)	2.84(8)	2.99(22)	3.11(40)	3.31(38)	3.95(51)	
7/2	3.509	3.48(25)	3.68(36)	3.41(51)	3.14(9)		3.52(43)	3.96(47)	4.51(59)	
8/2	4.010	4.17(31)	4.25(43)				4.13(47)	4.58(49)	5.13(68)	
9/2	4.511	4.83(36)	4.88(52)				4.55(52)	5.18(59)		
10/2	5.014	5.46(38)	5.52(57)				5.09(54)	5.78(67)		
4/3	1.333	1.32(9)	1.27(14)	1.38(3)	1.33(5)	1.30(11)	1.37(17)	1.35(15)	1.45(12)	
5/3	1.666	1.67(12)	1.66(18)	1.68(4)	1.62(6)	1.66(14)	1.80(22)	1.72(20)	1.93(16)	
6/3	1.999	2.00(13)	2.06(22)	1.94(4)	1.89(6)	1.97(16)	2.17(27)	2.16(23)	2.45(21)	
7/3	2.333	2.36(16)	2.37(26)	2.23(33)	2.09(7)		2.46(29)	2.58(29)	2.79(25)	
8/3	2.666	2.84(20)	2.74(30)				2.88(31)	2.98(30)	3.18(29)	
9/3	3.000	3.28(23)	3.15(36)				3.17(35)	3.37(37)		
10/3	3.334	3.71(25)	3.56(40)				3.55(36)	3.76(42)		
5/4	1.249	1.27(10)	1.31(12)	1.22(3)	1.22(3)	1.28(12)	1.31(19)	1.27(14)	1.33(9)	
6/4	1.500	1.51(11)	1.62(15)	1.41(2)	1.42(4)	1.52(14)	1.58(23)	1.59(17)	1.69(12)	
7/4	1.750	1.79(13)	1.87(18)	1.62(24)	1.58(4)		1.79(25)	1.91(21)	1.93(14)	
8/4	2.000	2.15(16)	2.16(21)				2.09(29)	2.20(22)	2.20(17)	
9/4	2.250	2.49(18)	2.49(25)				2.31(31)	2.49(27)		
10/4	2.500	2.81(20)	2.81(28)				2.58(33)	2.78(30)		
6/5	1.200	1.19(9)	1.24(12)	1.15(2)	1.16(3)	1.19(11)	1.20(18)	1.26(14)	1.27(9)	
7/5	1.401	1.41(11)	1.43(14)	1.33(20)	1.29(3)		1.36(20)	1.50(17)	1.45(11)	
8/5	1.601	1.70(14)	1.65(16)				1.60(22)	1.74(18)	1.65(13)	
9/5	1.801	1.96(16)	1.90(20)				1.76(25)	1.96(21)		
10/5	2.001	2.22(17)	2.15(22)				1.97(26)	2.19(24)		
7/6	1.167	1.18(9)	1.15(11)	1.15(17)	1.11(2)		1.13(16)	1.20(13)	1.14(9)	
8/6	1.334	1.42(11)	1.33(13)				1.33(18)	1.38(13)	1.30(11)	
9/6	1.500	1.65(13)	1.53(15)				1.46(20)	1.56(16)		
10/6	1.667	1.86(14)	1.73(17)				1.64(22)	1.74(18)		
8/7	1.143	1.20(9)	1.16(11)				1.17(15)	1.16(12)	1.14(10)	
9/7	1.286	1.39(11)	1.33(14)				1.29(17)	1.31(14)		
10/7	1.429	1.57(11)	1.50(15)				1.45(18)	1.46(16)		
9/8	1.125	1.16(9)	1.15(12)				1.10(14)	1.13(11)		
10/8	1.250	1.31(10)	1.30(13)				1.23(15)	1.26(12)		
10/9	1.111	1.13(9)	1.13(12)				1.12(13)	1.12(12)		

Table 5: Average eigenvalue ratios in the $\nu = 1$ sector in RMT and the A_i and B_i lattices.

j/k	RMT	$B_1(S)$	$B_2(S)$	$B_1(F)$	$B_2(F)$	$A_1(S)$	$A_2(S)$	$A_3(S)$	$A_4(S)$	$A_5(S)$
2/1	1.761	1.73(14)	1.55(42)	1.85(9)	1.82(15)	1.79(14)	1.77(11)	1.96(13)	1.87(40)	1.57(78)
3/1	2.500	2.53(21)	2.32(57)	2.75(13)	2.60(20)	2.49(18)	2.54(16)	2.89(24)	2.82(56)	2.4(1.2)
4/1	3.239	3.33(24)	2.96(70)	3.65(18)	3.33(25)	3.30(25)	3.68(31)	3.75(26)	3.35(67)	3.1(1.5)
5/1	3.953	3.99(28)	3.77(85)	4.37(21)	4.05(30)	4.11(30)	4.42(33)	4.71(32)	4.34(88)	4.0(1.9)
6/1	4.680	4.80(34)	4.5(1.0)		4.59(34)		5.19(38)	5.38(51)	5.3(1.1)	5.0(2.3)
7/1	5.404	5.61(40)	5.3(1.2)				6.06(40)	6.44(61)	6.3(1.2)	5.8(2.6)
8/1	6.129	6.45(46)	6.1(1.4)				6.78(42)	7.44(77)	7.0(1.3)	6.5(3.0)
9/1	6.853	7.25(52)	6.8(1.5)				7.60(47)	8.21(79)		7.3(3.5)
10/1	7.578	8.15(59)	7.5(1.6)				8.36(51)	9.06(83)		8.6(4.0)
3/2	1.420	1.46(11)	1.49(33)	1.48(4)	1.43(7)	1.39(9)	1.43(7)	1.47(10)	1.51(21)	1.50(42)
4/2	1.839	1.93(12)	1.90(40)	1.97(6)	1.83(9)	1.84(13)	2.07(16)	1.91(10)	1.79(26)	1.95(51)
5/2	2.245	2.31(14)	2.42(49)	2.36(7)	2.23(10)	2.29(15)	2.49(16)	2.40(12)	2.32(34)	2.56(63)
6/2	2.657	2.78(16)	2.92(59)		2.53(12)		2.92(19)	2.74(23)	2.84(40)	3.16(74)
7/2	3.069	3.25(20)	3.38(67)				3.42(19)	3.28(27)	3.39(43)	3.66(80)
8/2	3.480	3.73(22)	3.91(77)				3.82(20)	3.79(35)	3.73(48)	4.10(90)
9/2	3.892	4.20(26)	4.37(85)				4.28(22)	4.19(36)		4.7(1.1)
10/2	4.303	4.72(29)	4.79(93)				4.71(24)	4.62(37)		5.5(1.3)
4/3	1.296	1.32(8)	1.27(22)	1.33(4)	1.28(5)	1.32(8)	1.45(11)	1.30(9)	1.19(15)	1.30(32)
5/3	1.581	1.58(9)	1.63(26)	1.59(4)	1.56(5)	1.65(9)	1.74(12)	1.63(11)	1.54(20)	1.70(39)
6/3	1.872	1.90(11)	1.96(32)		1.77(6)		2.04(13)	1.86(18)	1.89(23)	2.10(46)
7/3	2.162	2.22(13)	2.27(36)				2.38(13)	2.23(21)	2.25(24)	2.44(49)
8/3	2.452	2.55(15)	2.62(42)				2.67(14)	2.58(27)	2.47(26)	2.73(55)
9/3	2.741	2.87(17)	2.93(46)				2.99(15)	2.84(28)		3.10(71)
10/3	3.031	3.23(20)	3.21(50)				3.29(17)	3.14(29)		3.63(80)
5/4	1.221	1.20(5)	1.28(19)	1.20(4)	1.22(4)	1.25(8)	1.20(10)	1.25(6)	1.29(17)	1.31(27)
6/4	1.445	1.44(7)	1.54(23)		1.38(5)		1.41(12)	1.43(12)	1.59(19)	1.62(31)
7/4	1.668	1.68(8)	1.78(26)				1.65(13)	1.71(14)	1.89(20)	1.87(33)
8/4	1.892	1.93(9)	2.06(30)				1.84(14)	1.98(19)	2.08(22)	2.10(37)
9/4	2.116	2.17(11)	2.30(33)				2.06(16)	2.19(19)		2.38(49)
10/4	2.340	2.44(12)	2.52(36)				2.27(17)	2.41(19)		2.79(55)
6/5	1.184	1.20(5)	1.21(16)		1.13(3)		1.17(9)	1.14(10)	1.23(16)	1.23(21)
7/5	1.367	1.41(6)	1.40(18)				1.37(10)	1.37(11)	1.46(16)	1.43(21)
8/5	1.550	1.62(7)	1.61(21)				1.53(10)	1.58(15)	1.61(18)	1.60(24)
9/5	1.734	1.82(8)	1.80(23)				1.72(11)	1.74(15)		1.82(34)
10/5	1.917	2.04(9)	1.98(25)				1.89(12)	1.92(15)		2.13(37)
7/6	1.155	1.17(5)	1.16(15)				1.17(8)	1.20(13)	1.19(12)	1.16(15)
8/6	1.310	1.34(6)	1.34(17)				1.31(8)	1.38(16)	1.31(14)	1.30(17)
9/6	1.464	1.51(7)	1.50(19)				1.46(9)	1.53(17)		1.47(25)
10/6	1.619	1.70(8)	1.64(20)				1.61(10)	1.69(18)		1.73(27)
8/7	1.134	1.15(5)	1.16(15)				1.12(6)	1.16(13)	1.10(10)	1.12(12)
9/7	1.268	1.29(6)	1.29(16)				1.25(7)	1.28(14)		1.27(19)
10/7	1.402	1.45(7)	1.42(17)				1.38(8)	1.41(15)		1.49(20)
9/8	1.118	1.12(5)	1.12(14)				1.12(6)	1.10(13)		1.13(17)
10/8	1.236	1.26(6)	1.23(15)				1.23(6)	1.22(14)		1.33(18)
10/9	1.106	1.12(5)	1.10(13)				1.10(5)	1.10(12)		1.17(20)

Table 6: Average eigenvalue ratios in the $\nu = 2$ sector in RMT and the A_i and B_i lattices.

j/k	RMT	$B_1(S)$	$B_2(S)$	$B_1(F)$	$B_2(F)$	$A_1(S)$	$A_2(S)$	$A_3(S)$	$A_4(S)$	$A_5(S)$
2/1	1.617	1.63(15)	1.73(18)	1.68(11)	1.67(11)	1.61(10)	1.60(11)	1.67(13)	2.31(62)	1.49(8)
3/1	2.208	2.25(22)	2.32(20)	2.30(15)	2.20(12)	2.15(13)	2.23(17)	2.35(18)	3.57(75)	1.93(18)
4/1	2.787	2.82(28)	2.92(25)	2.91(19)	2.61(15)	2.79(16)	2.88(21)	3.09(22)	4.40(84)	2.62(11)
5/1	3.363	3.44(33)	3.51(31)	3.34(20)	3.03(17)	3.41(20)	3.47(27)	3.73(27)	5.9(1.1)	3.01(13)
6/1	3.936	4.03(40)	4.16(32)		3.43(19)		4.17(31)	4.32(32)	6.7(1.3)	3.74(21)
7/1	4.506	4.70(46)	4.83(39)				4.86(36)	4.94(39)	7.4(1.4)	4.26(25)
8/1	5.077	5.35(50)	5.45(44)				5.48(40)	5.59(41)		4.87(41)
9/1	5.647	5.95(55)	6.13(47)				6.08(42)	6.35(47)		5.33(31)
10/1	6.216	6.56(61)	6.79(53)				6.74(44)	6.93(50)		5.74(38)
3/2	1.365	1.38(8)	1.34(13)	1.37(7)	1.32(6)	1.34(6)	1.39(9)	1.41(9)	1.54(36)	1.29(12)
4/2	1.723	1.72(10)	1.69(15)	1.74(7)	1.56(7)	1.74(8)	1.79(11)	1.85(11)	1.90(41)	1.76(7)
5/2	2.079	2.10(11)	2.03(19)	1.99(7)	1.82(8)	2.12(10)	2.17(15)	2.24(13)	2.56(55)	2.02(8)
6/2	2.433	2.47(15)	2.41(21)		2.05(9)		2.60(17)	2.59(15)	2.92(64)	2.50(13)
7/2	2.786	2.87(16)	2.80(25)				3.03(19)	2.96(20)	3.21(68)	2.85(16)
8/2	3.139	3.27(17)	3.16(28)				3.42(22)	3.35(20)		3.26(26)
9/2	3.491	3.64(18)	3.55(30)				3.80(23)	3.81(23)		3.57(19)
10/2	3.843	4.01(20)	3.93(33)				4.20(23)	4.15(24)		3.84(24)
4/3	1.263	1.25(8)	1.26(9)	1.27(6)	1.19(3)	1.30(6)	1.29(9)	1.31(8)	1.23(16)	1.36(12)
5/3	1.523	1.53(9)	1.51(11)	1.45(6)	1.38(3)	1.59(7)	1.56(12)	1.59(9)	1.65(22)	1.56(14)
6/3	1.783	1.79(12)	1.79(11)		1.56(4)		1.87(13)	1.84(11)	1.89(26)	1.94(19)
7/3	2.041	2.09(13)	2.08(14)				2.18(15)	2.10(14)	2.08(27)	2.21(21)
8/3	2.300	2.38(14)	2.35(15)				2.46(17)	2.38(14)		2.53(29)
9/3	2.558	2.65(14)	2.64(16)				2.73(18)	2.70(16)		2.77(27)
10/3	2.816	2.92(16)	2.92(18)				3.02(18)	2.94(17)		2.98(30)
5/4	1.206	1.22(8)	1.20(9)	1.15(4)	1.16(3)	1.22(5)	1.21(9)	1.21(6)	1.34(14)	1.15(3)
6/4	1.412	1.43(10)	1.43(8)		1.31(4)		1.45(10)	1.40(8)	1.53(17)	1.42(6)
7/4	1.617	1.67(11)	1.66(10)				1.69(11)	1.60(10)	1.68(16)	1.62(8)
8/4	1.821	1.90(12)	1.87(12)				1.91(13)	1.81(10)		1.86(14)
9/4	2.026	2.11(12)	2.10(12)				2.12(13)	2.06(11)		2.03(9)
10/4	2.230	2.33(14)	2.33(13)				2.34(13)	2.24(12)		2.19(12)
6/5	1.170	1.17(7)	1.19(8)		1.13(3)		1.20(9)	1.16(6)	1.14(13)	1.24(6)
7/5	1.340	1.37(8)	1.38(9)				1.40(10)	1.32(8)	1.25(13)	1.41(7)
8/5	1.510	1.55(8)	1.55(10)				1.58(11)	1.50(8)		1.62(12)
9/5	1.679	1.73(9)	1.75(11)				1.75(12)	1.70(10)		1.77(8)
10/5	1.849	1.91(10)	1.93(12)				1.94(12)	1.86(10)		1.90(11)
7/6	1.145	1.16(8)	1.16(6)				1.17(8)	1.14(7)	1.10(12)	1.14(7)
8/6	1.290	1.33(8)	1.31(7)				1.32(9)	1.29(7)		1.30(11)
9/6	1.435	1.48(9)	1.47(7)				1.46(9)	1.47(8)		1.42(8)
10/6	1.579	1.63(10)	1.63(8)				1.62(10)	1.60(9)		1.54(10)
8/7	1.127	1.14(7)	1.13(6)				1.13(7)	1.13(7)		1.14(10)
9/7	1.253	1.27(7)	1.27(7)				1.25(8)	1.29(8)		1.25(8)
10/7	1.379	1.40(8)	1.41(7)				1.39(8)	1.40(9)		1.35(9)
9/8	1.112	1.11(6)	1.12(6)				1.11(7)	1.14(6)		1.09(9)
10/8	1.224	1.23(6)	1.25(6)				1.23(7)	1.24(7)		1.18(11)
10/9	1.101	1.10(5)	1.11(5)				1.11(6)	1.09(6)		1.08(7)

Table 7: Average eigenvalue ratios in the $\nu = 3$ sector in RMT and the A_i and B_i lattices.

j/k	RMT	$B_1(S)$	$B_2(S)$	$B_1(F)$	$B_2(F)$	$A_1(S)$	$A_2(S)$	$A_3(S)$	$A_4(S)$	$A_5(S)$
2/1	1.529	1.41(7)	1.35(15)	1.48(12)	1.52(12)	1.58(21)	1.67(15)	1.51(12)	1.39(32)	
3/1	2.025	1.91(9)	1.96(25)	1.99(16)	1.97(14)	2.07(27)	1.89(21)	2.09(15)	1.89(45)	
4/1	2.510	2.46(11)	2.39(31)	2.50(17)	2.38(18)	2.58(33)	2.40(29)	2.58(19)	2.33(51)	
5/1	2.989	3.02(13)	2.86(37)		2.68(22)		2.92(29)	3.03(24)	2.78(59)	
6/1	3.465	3.58(17)	3.41(43)				3.61(40)	3.37(25)	3.02(64)	
7/1	3.940	4.07(18)	3.89(46)				4.00(41)	4.02(28)	3.61(79)	
8/1	4.415	4.56(21)	4.44(53)				4.49(44)	4.47(30)		
9/1	4.886	5.16(23)	4.99(60)				4.99(45)	4.97(33)		
10/1	5.357	5.95(32)	5.57(68)							
3/2	1.324	1.35(6)	1.45(11)	1.35(10)	1.29(5)	1.31(14)	1.14(13)	1.39(9)	1.37(32)	
4/2	1.642	1.75(8)	1.77(15)	1.69(10)	1.56(8)	1.63(16)	1.44(18)	1.71(11)	1.68(35)	
5/2	1.955	2.14(9)	2.12(18)		1.76(10)		1.75(18)	2.01(14)	2.00(40)	
6/2	2.267	2.54(12)	2.53(21)				2.16(25)	2.24(14)	2.18(44)	
7/2	2.577	2.89(12)	2.88(19)				2.40(26)	2.66(15)	2.60(55)	
8/2	2.888	3.24(14)	3.29(23)				2.69(28)	2.97(17)		
9/2	3.196	3.66(16)	3.70(25)				2.99(29)	3.29(18)		
10/2	3.505	4.22(22)	4.14(30)							
4/3	1.240	1.29(5)	1.22(12)	1.26(8)	1.21(5)	1.25(12)	1.26(17)	1.23(7)	1.23(27)	
5/3	1.476	1.59(6)	1.46(14)		1.36(7)		1.54(18)	1.45(9)	1.47(31)	
6/3	1.712	1.88(8)	1.74(17)				1.91(25)	1.61(9)	1.60(34)	
7/3	1.946	2.14(8)	1.99(17)				2.11(26)	1.92(10)	1.91(42)	
8/3	2.181	2.39(10)	2.27(19)				2.37(28)	2.14(11)		
9/3	2.413	2.71(11)	2.55(22)				2.63(29)	2.38(11)		
10/3	2.646	3.12(15)	2.85(25)							
5/4	1.191	1.23(5)	1.20(12)		1.13(7)		1.22(16)	1.18(8)	1.19(23)	
6/4	1.381	1.45(6)	1.43(15)				1.51(21)	1.31(7)	1.30(25)	
7/4	1.570	1.65(6)	1.63(15)				1.67(22)	1.56(8)	1.55(31)	
8/4	1.759	1.85(7)	1.86(17)				1.87(24)	1.74(9)		
9/4	1.947	2.10(8)	2.09(19)				2.08(26)	1.93(9)		
10/4	2.135	2.41(12)	2.33(22)							
6/5	1.159	1.19(4)	1.19(12)				1.24(15)	1.11(7)	1.09(20)	
7/5	1.318	1.35(5)	1.36(12)				1.37(15)	1.33(8)	1.30(25)	
8/5	1.477	1.51(5)	1.55(14)				1.54(17)	1.48(9)		
9/5	1.635	1.71(6)	1.75(16)				1.71(17)	1.64(9)		
10/5	1.793	1.97(9)	1.95(18)							
7/6	1.137	1.14(4)	1.14(10)				1.11(14)	1.19(6)	1.19(23)	
8/6	1.274	1.27(5)	1.30(11)				1.24(15)	1.33(7)		
9/6	1.410	1.44(6)	1.46(13)				1.38(16)	1.47(7)		
10/6	1.546	1.66(8)	1.63(15)							
8/7	1.121	1.12(4)	1.14(9)				1.12(13)	1.11(5)		
9/7	1.240	1.27(5)	1.28(10)				1.25(13)	1.24(5)		
10/7	1.360	1.46(7)	1.43(11)							
9/8	1.107	1.13(4)	1.12(9)				1.11(11)	1.11(5)		
10/8	1.214	1.30(6)	1.26(10)							
10/9	1.097	1.15(5)	1.12(9)							

Table 8: Average eigenvalue ratios in the $\nu = 4$ sector in RMT and the A_i and B_i lattices.

j/k	RMT	$B_1(S)$	$B_2(S)$	$B_1(F)$	$B_2(F)$	$A_1(S)$	$A_2(S)$	$A_3(S)$	$A_4(S)$	$A_5(S)$
2/1	1.465	1.53(8)	1.45(9)	1.42(24)	1.41(24)	1.45(9)	1.35(10)	1.47(7)	1.46(13)	1.45(12)
3/1	1.897	1.99(12)	1.99(12)	1.85(31)	1.81(29)	1.97(13)	1.73(11)	1.88(8)	1.88(15)	1.91(14)
4/1	2.316	2.55(16)	2.45(14)	2.21(35)	2.14(31)	2.33(14)	2.17(14)	2.27(10)	2.30(18)	2.30(17)
5/1	2.729	3.02(17)	2.94(17)		2.25(44)		2.55(17)	2.84(16)	2.71(21)	2.68(20)
6/1	3.139	3.47(21)	3.43(20)				2.93(18)	3.27(18)	3.12(23)	3.08(22)
7/1	3.547	3.92(23)	3.90(23)				3.29(20)	3.66(20)		3.51(25)
8/1	3.952	4.47(26)	4.46(26)				3.73(22)	4.07(21)		3.84(26)
9/1	4.357	4.92(28)	4.91(28)				4.13(24)	4.43(23)		4.22(28)
10/1	4.760	5.53(37)	5.41(33)							4.56(31)
3/2	1.295	1.30(7)	1.37(8)	1.30(16)	1.28(18)	1.36(8)	1.28(10)	1.28(4)	1.29(9)	1.32(8)
4/2	1.581	1.67(10)	1.69(9)	1.55(17)	1.51(18)	1.61(9)	1.61(13)	1.54(5)	1.58(11)	1.59(10)
5/2	1.863	1.97(11)	2.03(11)		1.60(29)		1.90(15)	1.93(9)	1.85(12)	1.85(11)
6/2	2.143	2.26(13)	2.36(13)				2.17(17)	2.22(10)	2.14(14)	2.12(12)
7/2	2.421	2.56(15)	2.69(15)				2.44(18)	2.49(11)		2.42(14)
8/2	2.698	2.92(17)	3.08(17)				2.77(20)	2.77(12)		2.65(15)
9/2	2.974	3.21(18)	3.38(19)				3.07(22)	3.01(13)		2.91(16)
10/2	3.250	3.61(24)	3.73(22)							3.14(17)
4/3	1.221	1.28(8)	1.23(6)	1.19(12)	1.18(13)	1.18(7)	1.25(9)	1.21(3)	1.22(7)	1.21(7)
5/3	1.438	1.52(9)	1.48(7)		1.25(22)		1.48(10)	1.51(7)	1.44(8)	1.40(7)
6/3	1.654	1.74(11)	1.72(9)				1.69(11)	1.74(8)	1.66(9)	1.61(8)
7/3	1.869	1.97(12)	1.96(10)				1.90(12)	1.94(8)		1.84(9)
8/3	2.083	2.24(14)	2.24(12)				2.16(13)	2.16(9)		2.01(10)
9/3	2.296	2.47(14)	2.46(12)				2.39(15)	2.35(9)		2.21(10)
10/3	2.509	2.78(19)	2.71(15)							2.38(11)
5/4	1.178	1.18(7)	1.20(5)		1.06(16)		1.18(8)	1.25(6)	1.18(6)	1.16(6)
6/4	1.355	1.36(9)	1.40(7)				1.35(9)	1.44(6)	1.36(7)	1.34(7)
7/4	1.531	1.54(10)	1.59(8)				1.52(10)	1.61(6)		1.53(8)
8/4	1.706	1.75(11)	1.82(9)				1.72(11)	1.79(7)		1.67(8)
9/4	1.881	1.93(12)	2.00(9)				1.91(12)	1.95(7)		1.83(8)
10/4	2.055	2.17(16)	2.21(11)							1.98(9)
6/5	1.150	1.15(7)	1.16(5)				1.15(8)	1.15(7)	1.15(5)	1.15(5)
7/5	1.299	1.30(8)	1.32(6)				1.29(8)	1.29(7)		1.31(6)
8/5	1.448	1.48(9)	1.52(7)				1.46(9)	1.43(8)		1.44(6)
9/5	1.596	1.63(9)	1.67(7)				1.62(10)	1.56(8)		1.58(7)
10/5	1.744	1.83(12)	1.84(9)							1.70(7)
7/6	1.130	1.13(7)	1.14(6)				1.12(7)	1.12(6)		1.14(5)
8/6	1.259	1.29(8)	1.30(6)				1.28(8)	1.24(6)		1.25(5)
9/6	1.388	1.42(9)	1.43(7)				1.41(8)	1.35(7)		1.37(5)
10/6	1.516	1.59(11)	1.58(8)							1.48(6)
8/7	1.114	1.14(7)	1.14(6)				1.13(7)	1.11(5)		1.09(4)
9/7	1.228	1.25(7)	1.26(6)				1.26(7)	1.21(6)		1.20(4)
10/7	1.342	1.41(10)	1.39(7)							1.30(5)
9/8	1.102	1.10(7)	1.10(5)				1.11(6)	1.09(5)		1.10(4)
10/8	1.204	1.24(9)	1.21(6)							1.19(4)
10/9	1.093	1.12(8)	1.10(6)							1.08(3)

Table 9: Average eigenvalue ratios in the $\nu = 5$ sector in RMT and the A_i and B_i lattices.

j/k	RMT	$B_1(S)$	$B_2(S)$	$B_1(F)$	$B_2(F)$	$A_1(S)$	$A_2(S)$	$A_3(S)$	$A_4(S)$	$A_5(S)$
2/1	1.417	1.44(10)	1.50(14)			1.44(12)	1.40(18)	1.47(21)		
3/1	1.801	1.83(13)	1.89(16)			1.82(14)	1.89(21)	1.84(24)		
4/1	2.172	2.26(16)	2.25(19)				2.22(27)	2.36(31)		
5/1	2.537	2.67(17)	2.67(23)				2.70(30)	2.62(38)		
6/1	2.898	3.08(20)	3.17(25)				3.06(31)	3.05(52)		
7/1	3.256	3.59(23)	3.64(30)				3.45(34)	3.28(48)		
8/1	3.612	4.00(25)	4.13(35)				3.90(35)	3.72(48)		
9/1	3.967	4.53(29)	4.48(41)							
10/1	4.323	4.97(31)	4.86(43)							
3/2	1.271	1.27(7)	1.26(9)			1.26(8)	1.35(19)	1.25(17)		
4/2	1.533	1.57(8)	1.50(11)				1.59(23)	1.60(21)		
5/2	1.791	1.85(8)	1.77(13)				1.93(27)	1.78(26)		
6/2	2.046	2.13(10)	2.11(14)				2.19(29)	2.07(35)		
7/2	2.298	2.48(11)	2.42(16)				2.46(32)	2.23(33)		
8/2	2.549	2.77(12)	2.75(19)				2.78(34)	2.53(33)		
9/2	2.800	3.14(14)	2.98(24)							
10/2	3.051	3.44(14)	3.24(24)							
4/3	1.206	1.24(7)	1.19(8)				1.18(16)	1.28(16)		
5/3	1.409	1.46(7)	1.41(9)				1.43(18)	1.42(19)		
6/3	1.609	1.68(8)	1.67(9)				1.62(19)	1.65(27)		
7/3	1.808	1.96(9)	1.92(11)				1.83(21)	1.78(24)		
8/3	2.006	2.18(10)	2.18(13)				2.06(22)	2.02(24)		
9/3	2.203	2.47(12)	2.37(17)							
10/3	2.400	2.71(13)	2.57(17)							
5/4	1.168	1.18(5)	1.19(8)				1.22(16)	1.11(15)		
6/4	1.334	1.36(6)	1.41(8)				1.38(17)	1.29(21)		
7/4	1.499	1.58(7)	1.62(9)				1.55(19)	1.39(19)		
8/4	1.663	1.77(7)	1.84(11)				1.75(20)	1.58(19)		
9/4	1.827	2.00(8)	1.99(14)							
10/4	1.990	2.19(9)	2.16(14)							
6/5	1.142	1.15(4)	1.19(7)				1.13(13)	1.17(20)		
7/5	1.284	1.35(5)	1.36(8)				1.28(14)	1.25(19)		
8/5	1.424	1.50(5)	1.55(9)				1.44(15)	1.42(19)		
9/5	1.564	1.70(6)	1.68(12)							
10/5	1.704	1.86(6)	1.82(12)							
7/6	1.124	1.16(4)	1.15(5)				1.13(12)	1.07(19)		
8/6	1.246	1.30(4)	1.30(7)				1.27(12)	1.22(19)		
9/6	1.369	1.47(5)	1.42(9)							
10/6	1.492	1.61(5)	1.54(9)							
8/7	1.109	1.12(3)	1.13(6)				1.13(10)	1.13(15)		
9/7	1.218	1.26(4)	1.23(8)							
10/7	1.328	1.38(4)	1.34(8)							
9/8	1.098	1.13(3)	1.09(8)							
10/8	1.197	1.24(3)	1.18(7)							
10/9	1.090	1.10(3)	1.09(8)							

Table 10: Average eigenvalue ratios in the $\nu = 6$ sector in RMT and the A_i and B_i lattices.

j/k	RMT	$B_1(S)$	$B_2(S)$	$B_1(F)$	$B_2(F)$	$A_1(S)$	$A_2(S)$	$A_3(S)$	$A_4(S)$	$A_5(S)$
2/1	1.384	1.47(16)	1.47(14)			1.38(7)	1.39(9)	1.44(13)	1.39(20)	1.35(73)
3/1	1.732	1.76(17)	1.83(17)			1.79(9)	1.78(10)	1.80(15)	1.78(21)	1.70(87)
4/1	2.067	2.17(22)	2.20(20)			2.53(14)	2.12(15)	2.00(17)	2.18(25)	1.9(1.0)
5/1	2.395	2.57(25)	2.62(25)			2.87(18)	2.45(16)	2.40(21)	2.47(29)	2.1(1.1)
6/1	2.719	3.00(27)	3.08(27)			3.34(21)	2.77(22)	2.77(24)		2.6(1.3)
7/1	3.041	3.41(30)	3.50(30)			3.67(26)	3.12(25)	3.12(27)		2.9(1.4)
8/1	3.360	3.79(33)	3.90(34)			3.91(29)	3.44(26)	3.51(28)		3.2(1.4)
9/1	3.678	4.44(42)	4.49(37)							3.5(1.5)
10/1	3.995	4.85(46)	4.94(39)							3.8(1.6)
3/2	1.251	1.20(12)	1.24(11)			1.30(5)	1.28(6)	1.25(8)	1.28(17)	1.26(64)
4/2	1.493	1.48(15)	1.50(13)			1.84(8)	1.53(10)	1.39(9)	1.56(20)	1.42(74)
5/2	1.731	1.75(18)	1.78(16)			2.09(11)	1.76(10)	1.67(11)	1.77(24)	1.53(78)
6/2	1.965	2.04(19)	2.09(18)			2.43(13)	1.99(14)	1.93(14)		1.94(97)
7/2	2.197	2.32(21)	2.38(19)			2.67(18)	2.24(17)	2.17(15)		2.1(1.0)
8/2	2.428	2.58(24)	2.65(22)			2.84(20)	2.47(17)	2.44(14)		2.4(1.1)
9/2	2.658	3.02(29)	3.05(24)							2.6(1.1)
10/2	2.887	3.30(32)	3.35(25)							2.8(1.2)
4/3	1.193	1.24(12)	1.20(10)			1.41(6)	1.19(7)	1.11(7)	1.22(12)	1.12(55)
5/3	1.383	1.46(14)	1.43(13)			1.61(8)	1.38(7)	1.33(8)	1.39(14)	1.21(57)
6/3	1.570	1.71(14)	1.68(13)			1.87(10)	1.56(10)	1.54(10)		1.53(71)
7/3	1.756	1.94(16)	1.91(15)			2.06(13)	1.75(12)	1.74(11)		1.69(76)
8/3	1.940	2.15(18)	2.13(17)			2.19(15)	1.93(12)	1.95(9)		1.90(75)
9/3	2.124	2.53(22)	2.46(18)							2.04(77)
10/3	2.307	2.76(25)	2.70(18)							2.22(86)
5/4	1.159	1.18(11)	1.19(10)			1.14(7)	1.15(8)	1.20(8)	1.14(12)	1.08(53)
6/4	1.316	1.38(12)	1.40(11)			1.32(8)	1.30(10)	1.38(9)		1.37(66)
7/4	1.471	1.57(13)	1.59(12)			1.45(10)	1.47(12)	1.56(10)		1.51(71)
8/4	1.626	1.74(15)	1.77(14)			1.55(11)	1.62(12)	1.75(9)		1.69(71)
9/4	1.780	2.04(18)	2.04(14)							1.82(73)
10/4	1.933	2.23(20)	2.24(15)							1.98(81)
6/5	1.135	1.17(10)	1.18(10)			1.16(8)	1.13(8)	1.15(8)		1.27(60)
7/5	1.270	1.33(11)	1.34(11)			1.28(9)	1.28(10)	1.30(9)		1.40(64)
8/5	1.403	1.47(12)	1.49(12)			1.36(10)	1.40(10)	1.46(8)		1.57(63)
9/5	1.536	1.73(15)	1.72(13)							1.69(65)
10/5	1.668	1.89(17)	1.89(14)							1.84(73)
7/6	1.118	1.14(8)	1.14(8)			1.10(8)	1.13(10)	1.13(8)		1.10(49)
8/6	1.236	1.26(9)	1.27(10)			1.17(9)	1.24(10)	1.27(7)		1.24(48)
9/6	1.353	1.48(11)	1.46(10)							1.33(49)
10/6	1.469	1.62(13)	1.61(10)							1.45(55)
8/7	1.105	1.11(8)	1.12(8)			1.06(9)	1.10(9)	1.12(6)		1.12(42)
9/7	1.210	1.30(10)	1.28(8)							1.21(43)
10/7	1.314	1.42(11)	1.41(9)							1.31(48)
9/8	1.095	1.17(9)	1.15(8)							1.08(30)
10/8	1.189	1.28(10)	1.27(8)							1.17(35)
10/9	1.086	1.09(9)	1.10(6)							1.09(29)

Table 11: Average eigenvalue ratios in the $\nu = 7$ sector in RMT and the A_i and B_i lattices.

j/k	RMT	$B_1(S)$	$B_2(S)$	$B_1(F)$	$B_2(F)$	$A_1(S)$	$A_2(S)$	$A_3(S)$	$A_4(S)$	$A_5(S)$
2/1	1.353	1.40(9)	1.28(17)			1.39(16)	1.32(6)	1.37(13)	1.30(25)	
3/1	1.671	1.83(10)	1.60(20)				1.63(7)	1.73(31)	1.69(32)	
4/1	1.976	2.11(12)	2.02(25)				1.94(8)	2.16(33)	2.14(38)	
5/1	2.274	2.50(14)	2.40(30)				2.28(10)	2.39(33)	2.49(44)	
6/1	2.567	2.92(16)	2.69(34)				2.59(12)	2.70(40)		
7/1	2.859	3.24(17)	3.16(43)				2.87(14)	3.05(47)		
8/1	3.148	3.73(22)	3.73(50)							
9/1	3.435	4.10(26)	4.25(64)							
10/1	3.722	4.51(29)	4.50(63)							
3/2	1.236	1.30(6)	1.25(16)				1.24(4)	1.26(23)	1.30(20)	
4/2	1.461	1.51(7)	1.58(20)				1.47(4)	1.58(24)	1.64(23)	
5/2	1.681	1.78(8)	1.88(24)				1.73(5)	1.74(24)	1.91(26)	
6/2	1.898	2.08(10)	2.11(27)				1.96(7)	1.96(29)		
7/2	2.113	2.31(10)	2.47(34)				2.18(8)	2.22(35)		
8/2	2.327	2.66(14)	2.93(40)							
9/2	2.539	2.92(17)	3.33(50)							
10/2	2.751	3.22(18)	3.53(50)							
4/3	1.182	1.15(4)	1.26(15)				1.19(4)	1.25(27)	1.27(17)	
5/3	1.361	1.37(5)	1.51(18)				1.40(4)	1.38(29)	1.48(20)	
6/3	1.536	1.59(6)	1.69(20)				1.59(6)	1.55(33)		
7/3	1.710	1.77(6)	1.98(25)				1.76(6)	1.76(38)		
8/3	1.883	2.04(9)	2.34(29)							
9/3	2.055	2.24(11)	2.66(38)							
10/3	2.227	2.47(12)	2.82(37)							
5/4	1.151	1.19(5)	1.19(14)				1.18(3)	1.10(20)	1.17(14)	
6/4	1.299	1.38(6)	1.33(16)				1.33(5)	1.25(24)		
7/4	1.447	1.54(6)	1.57(20)				1.48(5)	1.41(28)		
8/4	1.593	1.77(8)	1.85(23)							
9/4	1.738	1.94(10)	2.11(30)							
10/4	1.883	2.14(11)	2.23(30)							
6/5	1.129	1.17(5)	1.12(13)				1.13(4)	1.13(20)		
7/5	1.257	1.30(5)	1.31(17)				1.26(4)	1.28(24)		
8/5	1.384	1.49(7)	1.55(20)							
9/5	1.511	1.64(8)	1.77(25)							
10/5	1.637	1.80(9)	1.87(25)							
7/6	1.114	1.11(4)	1.17(15)				1.11(4)	1.13(22)		
8/6	1.226	1.28(6)	1.39(18)							
9/6	1.338	1.41(7)	1.58(23)							
10/6	1.450	1.55(8)	1.67(22)							
8/7	1.101	1.15(5)	1.18(16)							
9/7	1.202	1.26(6)	1.35(20)							
10/7	1.302	1.39(7)	1.43(20)							
9/8	1.091	1.10(6)	1.14(17)							
10/8	1.183	1.21(7)	1.21(17)							
10/9	1.084	1.10(7)	1.06(17)							

Table 12: Average eigenvalue ratios in the $\nu = 8$ sector in RMT and the A_i and B_i lattices.

j/k	RMT	$B_1(S)$	$B_2(S)$	$B_1(F)$	$B_2(F)$	$A_1(S)$	$A_2(S)$	$A_3(S)$	$A_4(S)$	$A_5(S)$
2/1	1.328	1.34(10)	1.20(13)			1.35(9)	1.38(13)	1.35(14)		
3/1	1.623	1.68(12)	1.63(18)				1.70(17)	1.55(16)		
4/1	1.904	1.97(13)	1.87(20)				2.09(22)	1.79(19)		
5/1	2.178	2.28(14)	2.26(26)				1.80(27)	2.08(20)		
6/1	2.448	2.59(17)	2.59(26)				2.05(18)	2.38(22)		
7/1	2.714	2.98(19)	2.88(30)				2.42(19)	2.68(25)		
8/1	2.979	3.48(30)	3.18(35)							
9/1	3.242	3.74(32)	3.61(38)							
10/1	3.503	4.08(33)	3.87(39)							
3/2	1.222	1.26(9)	1.35(17)				1.23(12)	1.15(10)		
4/2	1.433	1.47(10)	1.56(19)				1.51(15)	1.33(12)		
5/2	1.640	1.70(11)	1.88(25)				1.30(19)	1.54(12)		
6/2	1.843	1.94(13)	2.16(26)				1.48(11)	1.75(13)		
7/2	2.043	2.23(15)	2.39(29)				1.75(12)	1.98(14)		
8/2	2.242	2.60(23)	2.65(33)							
9/2	2.441	2.79(25)	3.01(36)							
10/2	2.637	3.05(26)	3.22(38)							
4/3	1.173	1.17(8)	1.15(15)				1.23(13)	1.16(10)		
5/3	1.342	1.35(9)	1.39(19)				1.06(16)	1.34(10)		
6/3	1.508	1.54(10)	1.59(19)				1.21(10)	1.53(11)		
7/3	1.672	1.77(12)	1.77(22)				1.42(11)	1.72(12)		
8/3	1.835	2.06(18)	1.96(25)							
9/3	1.997	2.22(19)	2.22(27)							
10/3	2.158	2.42(20)	2.38(29)							
5/4	1.144	1.16(7)	1.21(16)				0.86(13)	1.16(9)		
6/4	1.285	1.31(8)	1.39(17)				0.98(9)	1.32(10)		
7/4	1.425	1.51(9)	1.54(19)				1.16(10)	1.49(11)		
8/4	1.564	1.77(15)	1.70(22)							
9/4	1.703	1.90(16)	1.93(24)							
10/4	1.840	2.07(17)	2.07(25)							
6/5	1.124	1.14(7)	1.15(15)				1.14(16)	1.14(7)		
7/5	1.246	1.31(8)	1.28(17)				1.35(18)	1.29(8)		
8/5	1.367	1.53(12)	1.41(19)							
9/5	1.488	1.64(13)	1.60(21)							
10/5	1.608	1.79(14)	1.71(22)							
7/6	1.109	1.15(7)	1.11(13)				1.18(6)	1.13(6)		
8/6	1.217	1.34(11)	1.23(15)							
9/6	1.324	1.44(12)	1.39(16)							
10/6	1.431	1.58(12)	1.49(17)							
8/7	1.098	1.17(10)	1.11(14)							
9/7	1.194	1.25(10)	1.26(15)							
10/7	1.291	1.37(11)	1.34(16)							
9/8	1.088	1.07(11)	1.13(14)							
10/8	1.176	1.17(11)	1.22(15)							
10/9	1.081	1.09(10)	1.07(12)							

Table 13: Average eigenvalue ratios in the $\nu = 9$ sector in RMT and the A_i and B_i lattices.

j/k	RMT	$B_1(S)$	$B_2(S)$	$B_1(F)$	$B_2(F)$	$A_1(S)$	$A_2(S)$	$A_3(S)$	$A_4(S)$	$A_5(S)$
2/1	1.309	1.35(10)	1.30(11)				1.39(8)	1.26(9)	1.36(11)	1.37(12)
3/1	1.583	1.74(13)	1.57(11)				1.71(9)	1.52(9)	1.62(13)	1.64(12)
4/1	1.845	2.09(15)	1.86(13)				1.96(10)	1.72(10)	1.90(14)	1.88(14)
5/1	2.099	2.40(17)	2.15(15)				2.31(12)	2.08(11)		2.10(16)
6/1	2.348	2.68(19)	2.49(16)				2.59(13)	2.31(12)		2.41(18)
7/1	2.594	3.00(22)	2.67(20)							2.63(19)
8/1	2.838	3.30(24)	2.97(22)							2.84(20)
9/1	3.081	3.68(27)	3.23(23)							3.06(22)
10/1	3.323	4.00(28)	3.46(25)							3.28(24)
3/2	1.210	1.29(8)	1.21(9)				1.23(7)	1.20(9)	1.19(7)	1.20(8)
4/2	1.410	1.54(9)	1.43(11)				1.42(7)	1.36(10)	1.40(8)	1.37(9)
5/2	1.604	1.77(10)	1.66(12)				1.66(9)	1.65(12)		1.54(11)
6/2	1.794	1.98(12)	1.92(14)				1.87(10)	1.83(12)		1.76(12)
7/2	1.982	2.22(14)	2.06(16)							1.93(13)
8/2	2.169	2.43(15)	2.29(18)							2.08(13)
9/2	2.355	2.72(16)	2.49(19)							2.24(14)
10/2	2.539	2.95(17)	2.67(20)							2.40(16)
4/3	1.165	1.20(7)	1.18(8)				1.15(5)	1.13(7)	1.17(6)	1.15(6)
5/3	1.326	1.38(7)	1.37(8)				1.35(6)	1.37(8)		1.28(7)
6/3	1.483	1.54(9)	1.58(9)				1.52(6)	1.52(8)		1.47(8)
7/3	1.639	1.72(10)	1.70(12)							1.61(8)
8/3	1.793	1.89(11)	1.89(13)							1.74(9)
9/3	1.946	2.11(12)	2.06(13)							1.87(9)
10/3	2.099	2.29(12)	2.20(14)							2.00(10)
5/4	1.138	1.15(6)	1.16(7)				1.18(5)	1.21(7)		1.12(6)
6/4	1.273	1.29(7)	1.34(8)				1.32(5)	1.34(7)		1.28(7)
7/4	1.406	1.44(8)	1.44(10)							1.40(7)
8/4	1.539	1.58(9)	1.60(11)							1.51(8)
9/4	1.670	1.77(10)	1.74(11)							1.63(8)
10/4	1.801	1.92(10)	1.86(12)							1.75(9)
6/5	1.119	1.12(6)	1.16(6)				1.12(5)	1.11(5)		1.14(6)
7/5	1.236	1.25(7)	1.24(8)							1.25(7)
8/5	1.352	1.37(8)	1.38(9)							1.35(7)
9/5	1.468	1.54(8)	1.50(9)							1.46(8)
10/5	1.583	1.67(8)	1.61(10)							1.56(8)
7/6	1.105	1.12(6)	1.07(7)							1.09(5)
8/6	1.209	1.23(7)	1.19(7)							1.18(6)
9/6	1.312	1.37(8)	1.30(8)							1.27(6)
10/6	1.415	1.49(8)	1.39(8)							1.36(7)
8/7	1.094	1.10(6)	1.11(8)							1.08(5)
9/7	1.188	1.23(7)	1.21(8)							1.16(5)
10/7	1.281	1.33(7)	1.30(9)							1.24(6)
9/8	1.086	1.12(6)	1.09(7)							1.08(5)
10/8	1.171	1.21(7)	1.17(8)							1.15(5)
10/9	1.078	1.09(6)	1.07(7)							1.07(5)

Table 14: Average eigenvalue ratios in the $\nu = 10$ sector in RMT and the A_i and B_i lattices.

j/k	RMT	$B_1(S)$	$B_2(S)$	$B_1(F)$	$B_2(F)$	$A_1(S)$	$A_2(S)$	$A_3(S)$	$A_4(S)$	$A_5(S)$
2/1	1.292	1.31(12)	1.36(18)				1.50(23)			
3/1	1.549	1.57(14)	1.76(22)				1.72(26)			
4/1	1.793	1.83(16)	2.05(26)				2.03(29)			
5/1	2.029	2.12(18)	2.31(27)				2.32(33)			
6/1	2.262	2.42(18)	2.62(31)				2.64(38)			
7/1	2.491	2.74(29)	2.80(32)							
8/1	2.719	2.93(28)	3.11(35)							
9/1	2.944	3.27(33)	3.41(38)							
10/1	3.169	3.49(33)	3.67(41)							
3/2	1.199	1.20(10)	1.29(14)				1.14(13)			
4/2	1.388	1.39(12)	1.51(16)				1.35(15)			
5/2	1.571	1.61(13)	1.70(17)				1.54(17)			
6/2	1.751	1.84(13)	1.93(19)				1.75(20)			
7/2	1.929	2.09(21)	2.06(19)							
8/2	2.105	2.23(20)	2.29(21)							
9/2	2.279	2.49(24)	2.52(23)							
10/2	2.453	2.66(24)	2.71(24)							
4/3	1.158	1.16(10)	1.16(12)				1.18(12)			
5/3	1.310	1.35(11)	1.32(12)				1.35(14)			
6/3	1.461	1.54(11)	1.49(14)				1.53(16)			
7/3	1.609	1.74(18)	1.59(14)							
8/3	1.756	1.86(17)	1.77(15)							
9/3	1.901	2.08(21)	1.94(17)							
10/3	2.046	2.22(20)	2.09(17)							
5/4	1.132	1.16(9)	1.13(10)				1.14(11)			
6/4	1.262	1.32(9)	1.28(12)				1.30(13)			
7/4	1.390	1.50(15)	1.37(12)							
8/4	1.517	1.60(14)	1.52(12)							
9/4	1.642	1.79(17)	1.67(14)							
10/4	1.768	1.91(17)	1.80(15)							
6/5	1.115	1.14(7)	1.13(9)				1.14(11)			
7/5	1.228	1.30(12)	1.21(9)							
8/5	1.340	1.38(12)	1.35(9)							
9/5	1.451	1.54(14)	1.48(10)							
10/5	1.562	1.65(14)	1.59(11)							
7/6	1.102	1.13(10)	1.07(8)							
8/6	1.202	1.21(9)	1.19(9)							
9/6	1.302	1.35(11)	1.30(10)							
10/6	1.401	1.44(11)	1.40(10)							
8/7	1.091	1.07(11)	1.11(7)							
9/7	1.182	1.19(13)	1.22(8)							
10/7	1.272	1.27(13)	1.31(8)							
9/8	1.083	1.12(12)	1.10(7)							
10/8	1.166	1.19(11)	1.18(7)							
10/9	1.076	1.07(11)	1.08(6)							

Table 15: Average eigenvalue ratios in the $\nu = 11$ sector in RMT and the A_i and B_i lattices.

j/k	RMT	$B_1(S)$	$B_2(S)$	$B_1(F)$	$B_2(F)$	$A_1(S)$	$A_2(S)$	$A_3(S)$	$A_4(S)$	$A_5(S)$
2/1	1.275	1.34(14)	1.30(10)			1.29(11)	1.30(11)	1.29(19)	1.47(8)	1.25(10)
3/1	1.518	1.62(16)	1.60(11)			1.54(12)	1.58(13)	1.50(21)	1.62(10)	1.43(14)
4/1	1.747	1.88(18)	1.90(13)			1.55(11)	1.79(14)	1.73(25)		1.67(19)
5/1	1.969	2.14(20)	2.22(16)			1.76(12)	2.02(16)	1.94(24)		1.83(24)
6/1	2.187	2.68(27)	2.46(19)							2.06(19)
7/1	2.401	2.92(29)	2.81(21)							2.26(17)
8/1	2.614	3.19(31)	3.08(24)							2.37(17)
9/1	2.825	3.48(32)	3.38(25)							2.56(18)
10/1	3.034	3.80(37)	3.65(29)							2.67(18)
3/2	1.190	1.21(11)	1.23(8)			1.20(10)	1.21(10)	1.17(19)	1.10(8)	1.15(11)
4/2	1.370	1.40(12)	1.46(9)			1.21(8)	1.37(11)	1.35(22)		1.34(15)
5/2	1.544	1.59(14)	1.70(12)			1.37(9)	1.55(13)	1.51(23)		1.46(19)
6/2	1.715	2.00(19)	1.89(13)							1.65(15)
7/2	1.883	2.18(21)	2.16(15)							1.81(14)
8/2	2.050	2.38(22)	2.36(17)							1.90(14)
9/2	2.215	2.59(23)	2.60(18)							2.05(14)
10/2	2.379	2.84(26)	2.81(21)							2.14(15)
4/3	1.151	1.16(9)	1.19(7)			1.01(7)	1.13(9)	1.16(18)		1.17(14)
5/3	1.297	1.32(10)	1.39(9)			1.14(7)	1.27(10)	1.29(18)		1.28(18)
6/3	1.441	1.65(15)	1.54(10)							1.44(15)
7/3	1.582	1.80(16)	1.76(11)							1.58(14)
8/3	1.722	1.97(16)	1.92(13)							1.66(15)
9/3	1.861	2.14(17)	2.11(13)							1.79(16)
10/3	1.999	2.35(20)	2.28(16)							1.87(16)
5/4	1.127	1.14(8)	1.17(7)			1.13(6)	1.13(9)	1.12(16)		1.10(17)
6/4	1.252	1.42(12)	1.29(8)							1.23(15)
7/4	1.374	1.55(12)	1.48(9)							1.35(15)
8/4	1.496	1.70(13)	1.62(10)							1.42(15)
9/4	1.617	1.85(13)	1.78(10)							1.53(16)
10/4	1.737	2.02(15)	1.92(13)							1.60(16)
6/5	1.111	1.25(10)	1.11(8)							1.13(15)
7/5	1.219	1.37(11)	1.27(9)							1.23(16)
8/5	1.328	1.49(11)	1.39(10)							1.30(16)
9/5	1.435	1.63(11)	1.52(10)							1.40(17)
10/5	1.541	1.78(13)	1.65(12)							1.46(18)
7/6	1.098	1.09(10)	1.15(8)							1.10(10)
8/6	1.195	1.19(10)	1.25(9)							1.15(10)
9/6	1.292	1.30(10)	1.37(9)							1.24(10)
10/6	1.387	1.42(12)	1.49(11)							1.30(10)
8/7	1.089	1.09(9)	1.09(8)							1.05(7)
9/7	1.176	1.19(9)	1.20(8)							1.13(7)
10/7	1.263	1.30(11)	1.30(10)							1.18(7)
9/8	1.081	1.09(8)	1.10(8)							1.08(7)
10/8	1.161	1.19(9)	1.19(9)							1.13(7)
10/9	1.074	1.09(8)	1.08(8)							1.05(6)

Table 16: Average eigenvalue ratios in the $\nu = 12$ sector in RMT and the A_i and B_i lattices.

j/k	RMT	$B_1(S)$	$B_2(S)$	$B_1(F)$	$B_2(F)$	$A_1(S)$	$A_2(S)$	$A_3(S)$	$A_4(S)$	$A_5(S)$
2/1	1.262	1.20(15)	1.29(14)			1.31(18)	1.32(13)	1.30(14)	1.16(29)	
3/1	1.492	1.46(17)	1.55(16)			1.31(16)	1.65(16)	1.64(19)		
4/1	1.708	1.69(20)	1.83(21)			1.58(16)	1.87(18)	1.84(21)		
5/1	1.918	1.88(22)	2.13(23)			1.84(21)	2.12(19)	2.07(23)		
6/1	2.123	2.57(31)	2.35(24)							
7/1	2.324	2.77(37)	2.57(26)							
8/1	2.524	3.04(48)	2.80(28)							
9/1	2.723	3.25(54)	3.04(31)							
10/1	2.919	3.52(53)	3.21(32)							
3/2	1.182	1.22(12)	1.20(12)			1.00(14)	1.25(10)	1.26(11)		
4/2	1.354	1.41(13)	1.43(15)			1.21(15)	1.42(12)	1.41(13)		
5/2	1.520	1.57(15)	1.66(16)			1.41(18)	1.61(12)	1.59(14)		
6/2	1.682	2.14(21)	1.83(17)							
7/2	1.842	2.31(27)	2.00(18)							
8/2	2.000	2.53(36)	2.18(19)							
9/2	2.157	2.72(41)	2.36(22)							
10/2	2.313	2.93(39)	2.50(23)							
4/3	1.145	1.15(9)	1.19(12)			1.20(11)	1.13(9)	1.12(11)		
5/3	1.286	1.29(10)	1.38(13)			1.40(15)	1.28(9)	1.26(12)		
6/3	1.423	1.76(16)	1.52(13)							
7/3	1.558	1.89(20)	1.66(14)							
8/3	1.692	2.07(28)	1.81(15)							
9/3	1.825	2.22(32)	1.96(17)							
10/3	1.957	2.40(30)	2.08(18)							
5/4	1.123	1.11(9)	1.16(13)			1.17(10)	1.13(8)	1.13(11)		
6/4	1.243	1.52(13)	1.28(13)							
7/4	1.361	1.64(17)	1.40(14)							
8/4	1.478	1.80(24)	1.52(15)							
9/4	1.594	1.93(27)	1.66(17)							
10/4	1.709	2.08(26)	1.75(18)							
6/5	1.107	1.36(12)	1.10(10)							
7/5	1.212	1.47(15)	1.20(11)							
8/5	1.316	1.61(22)	1.31(12)							
9/5	1.420	1.73(25)	1.42(13)							
10/5	1.522	1.87(23)	1.50(14)							
7/6	1.095	1.08(12)	1.09(9)							
8/6	1.189	1.18(16)	1.19(10)							
9/6	1.283	1.27(19)	1.29(11)							
10/6	1.375	1.37(18)	1.37(11)							
8/7	1.086	1.10(17)	1.09(9)							
9/7	1.171	1.18(19)	1.18(10)							
10/7	1.256	1.27(18)	1.25(10)							
9/8	1.079	1.07(19)	1.09(9)							
10/8	1.157	1.16(19)	1.15(9)							
10/9	1.072	1.08(19)	1.06(9)							

Table 17: Average eigenvalue ratios in the $\nu = 13$ sector in RMT and the A_i and B_i lattices.

j/k	RMT	$B_1(S)$	$B_2(S)$	$B_1(F)$	$B_2(F)$	$A_1(S)$	$A_2(S)$	$A_3(S)$	$A_4(S)$	$A_5(S)$
2/1	1.250	1.24(14)	1.30(19)			1.36(19)	1.33(11)	1.16(41)		
3/1	1.468	1.57(17)	1.58(27)			1.79(22)	1.55(13)			
4/1	1.674	1.88(20)	1.73(44)			2.13(29)	1.88(14)			
5/1	1.872	2.18(38)								
6/1	2.067	2.48(42)								
7/1	2.257	2.68(46)								
8/1	2.446	2.91(49)								
9/1	2.633	3.17(57)								
3/2	1.175	1.27(14)	1.22(28)			1.32(11)	1.17(10)			
4/2	1.339	1.52(17)	1.33(39)			1.56(16)	1.42(10)			
5/2	1.498	1.76(31)								
6/2	1.653	2.00(34)								
7/2	1.806	2.16(38)								
8/2	1.956	2.35(40)								
9/2	2.106	2.56(47)								
4/3	1.140	1.20(12)	1.09(33)			1.19(10)	1.21(8)			
5/3	1.275	1.38(24)								
6/3	1.407	1.58(27)								
7/3	1.537	1.71(29)								
8/3	1.666	1.85(31)								
9/3	1.793	2.02(36)								
5/4	1.119	1.16(20)								
6/4	1.235	1.32(22)								
7/4	1.349	1.43(24)								
8/4	1.461	1.55(26)								
9/4	1.573	1.69(30)								
6/5	1.104	1.14(25)								
7/5	1.206	1.23(27)								
8/5	1.306	1.34(29)								
9/5	1.406	1.46(33)								
7/6	1.092	1.08(23)								
8/6	1.183	1.17(25)								
9/6	1.274	1.28(28)								
8/7	1.083	1.09(23)								
9/7	1.166	1.18(27)								
9/8	1.077	1.09(24)								

Table 18: Average eigenvalue ratios in the $\nu = 14$ sector in RMT and the A_i and B_i lattices.

j/k	RMT	$B_1(S)$	$B_2(S)$	$B_1(F)$	$B_2(F)$	$A_1(S)$	$A_2(S)$	$A_3(S)$	$A_4(S)$	$A_5(S)$
2/1	1.240	1.32(10)	1.31(19)			1.19(11)	1.28(15)	1.48(16)	0.93(28)	1.16(23)
3/1	1.448	1.62(11)	1.55(21)			1.37(21)	1.48(16)	1.73(22)	1.12(26)	1.38(29)
4/1	1.644	1.88(12)	1.84(26)			1.66(20)	1.68(17)	1.94(23)	1.31(29)	1.50(28)
5/1	1.832	2.11(15)	2.11(30)						1.55(30)	1.60(31)
6/1	2.016	2.36(16)	2.30(32)						1.82(31)	1.72(33)
7/1	2.197	2.56(17)	2.56(35)						2.09(44)	1.88(34)
8/1	2.376	2.78(17)	2.72(37)						2.29(55)	2.00(35)
9/1	2.553	2.98(17)	2.98(36)						2.38(49)	2.15(37)
10/1	2.728		3.21(39)							2.29(41)
3/2	1.168	1.22(9)	1.19(16)			1.15(18)	1.16(10)	1.17(15)	1.22(44)	1.20(20)
4/2	1.325	1.42(10)	1.41(19)			1.39(17)	1.31(11)	1.31(16)	1.42(50)	1.30(19)
5/2	1.478	1.59(12)	1.61(22)						1.67(57)	1.38(21)
6/2	1.626	1.78(13)	1.76(24)						1.97(64)	1.49(23)
7/2	1.772	1.93(13)	1.96(25)						2.26(79)	1.62(23)
8/2	1.916	2.10(14)	2.08(27)						2.47(91)	1.73(22)
9/2	2.059	2.25(14)	2.28(26)						2.57(89)	1.86(23)
10/2	2.200		2.45(28)							1.98(27)
4/3	1.135	1.16(8)	1.19(15)			1.21(20)	1.14(8)	1.12(16)	1.16(34)	1.09(17)
5/3	1.265	1.30(10)	1.36(18)						1.38(39)	1.16(19)
6/3	1.392	1.45(10)	1.48(19)						1.62(43)	1.25(20)
7/3	1.517	1.58(11)	1.65(20)						1.86(54)	1.36(20)
8/3	1.641	1.71(11)	1.75(21)						2.03(64)	1.45(20)
9/3	1.763	1.84(11)	1.92(21)						2.12(61)	1.55(21)
10/3	1.884		2.07(22)							1.66(24)
5/4	1.115	1.12(8)	1.14(15)						1.18(32)	1.06(15)
6/4	1.227	1.25(8)	1.25(16)						1.39(35)	1.15(16)
7/4	1.337	1.36(8)	1.39(17)						1.60(45)	1.25(15)
8/4	1.445	1.47(8)	1.48(18)						1.75(54)	1.33(14)
9/4	1.553	1.58(8)	1.62(18)						1.82(51)	1.43(15)
10/4	1.660		1.74(19)							1.53(18)
6/5	1.100	1.12(8)	1.09(15)						1.17(28)	1.08(16)
7/5	1.199	1.21(8)	1.22(16)						1.35(36)	1.17(15)
8/5	1.297	1.32(9)	1.29(17)						1.48(43)	1.25(15)
9/5	1.393	1.41(9)	1.41(16)						1.54(40)	1.34(15)
10/5	1.489		1.52(17)							1.44(18)
7/6	1.090	1.09(7)	1.11(14)						1.15(29)	1.09(14)
8/6	1.178	1.18(7)	1.18(15)						1.26(35)	1.16(13)
9/6	1.266	1.27(7)	1.29(14)						1.31(32)	1.25(14)
10/6	1.353		1.39(15)							1.33(16)
8/7	1.081	1.08(6)	1.06(13)						1.09(33)	1.07(10)
9/7	1.162	1.16(6)	1.16(12)						1.14(31)	1.14(11)
10/7	1.242		1.25(13)							1.22(13)
9/8	1.075	1.07(5)	1.09(11)						1.04(31)	1.07(8)
10/8	1.148		1.18(12)							1.15(10)
10/9	1.069		1.08(9)							1.07(9)

Table 19: Average eigenvalue ratios in the $\nu = 15$ sector in RMT and the A_i and B_i lattices.

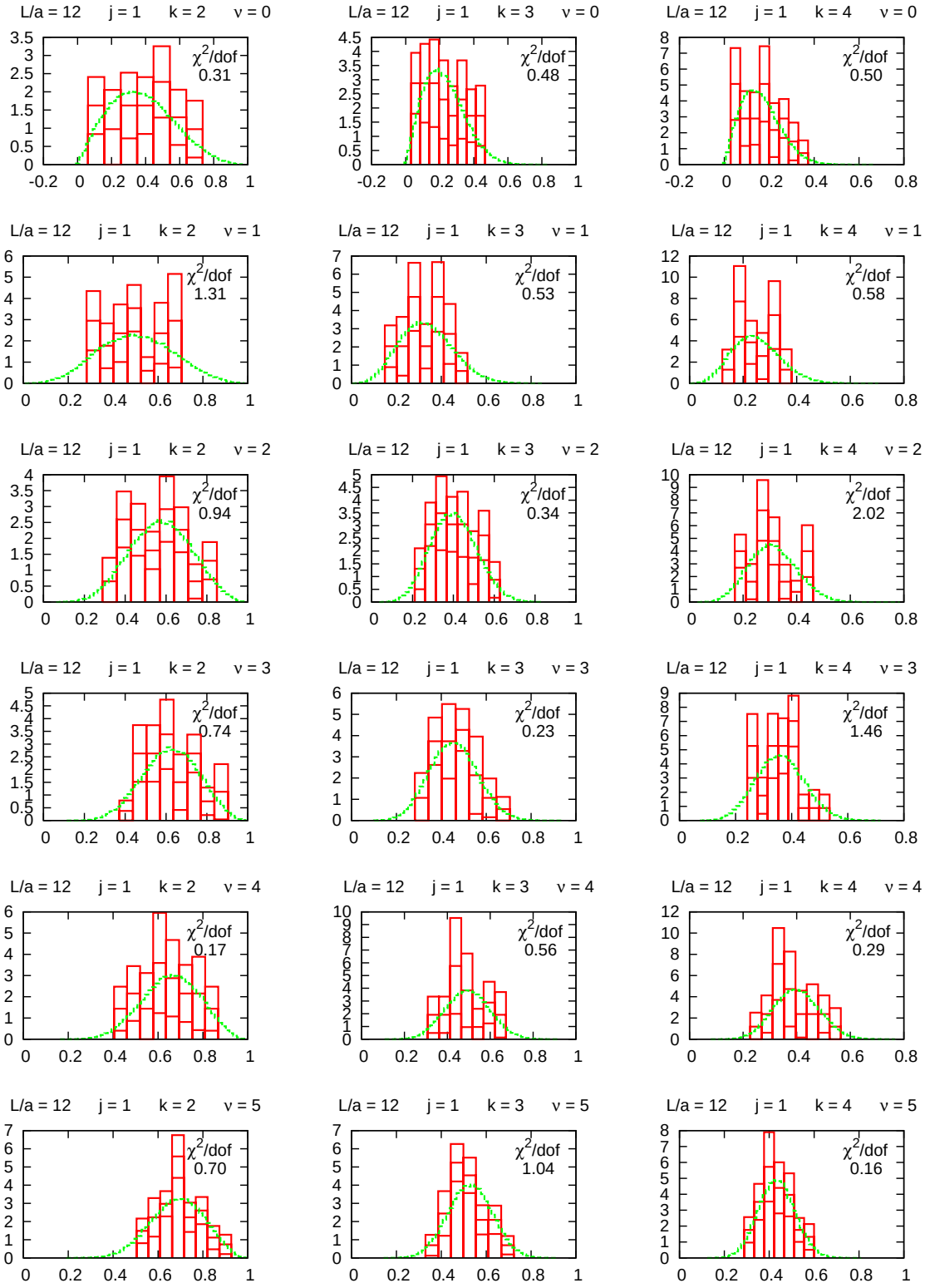

Figure 3: Distribution of the ratios λ_j/λ_k in the sectors $\nu = 0, 1, 2, 3, 4, 5$ for the A_1 lattice and sextet representation. The green (finer) histograms are from RMT, the red histograms are from the simulation including jackknife errors.

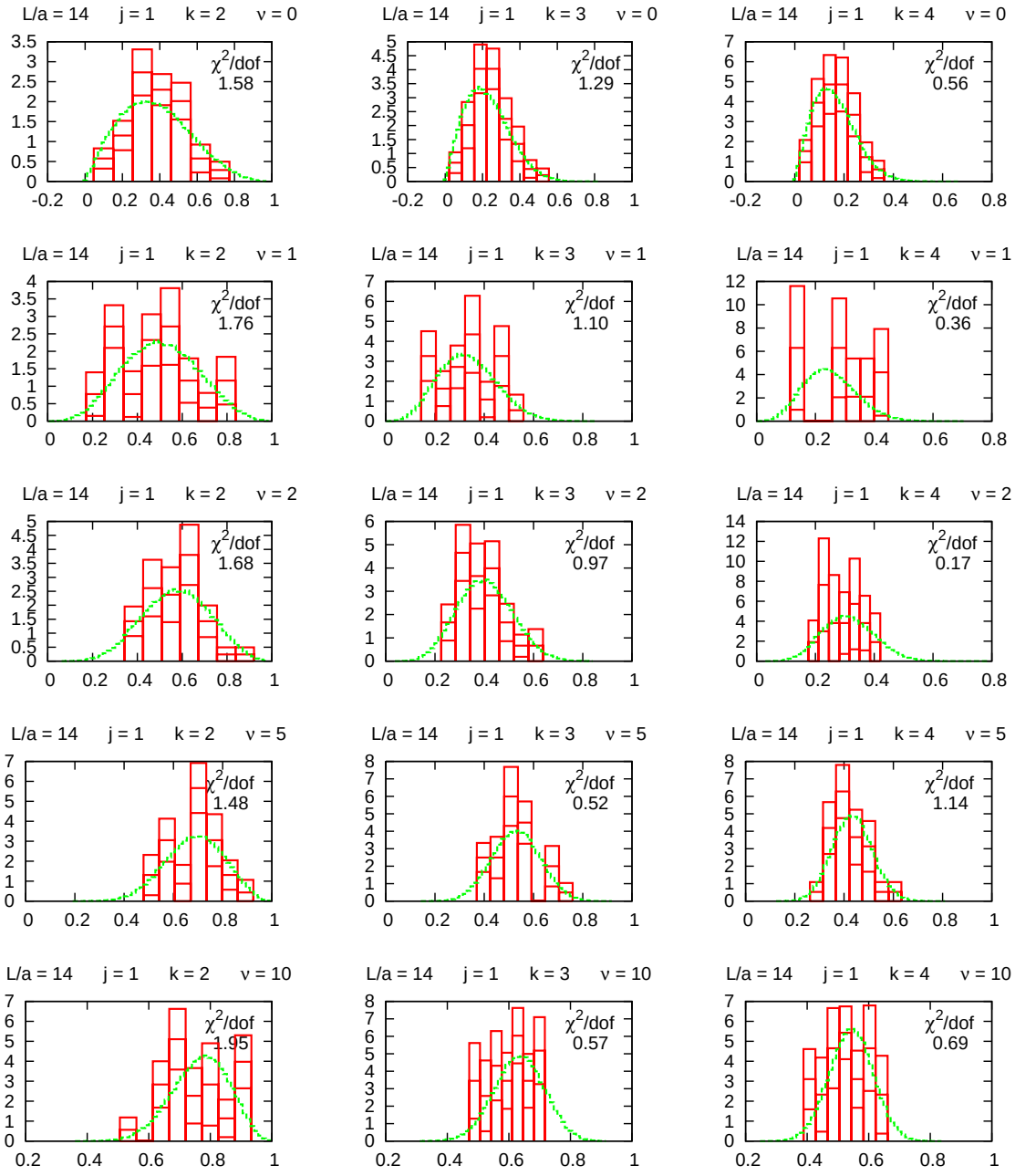

Figure 4: Distribution of the ratios λ_j/λ_k in the sectors $\nu = 0, 1, 2, 5, 10$ for the A_2 lattice and sextet representation. The green (finer) histograms are from RMT, the red histograms are from the simulation including jackknife errors.

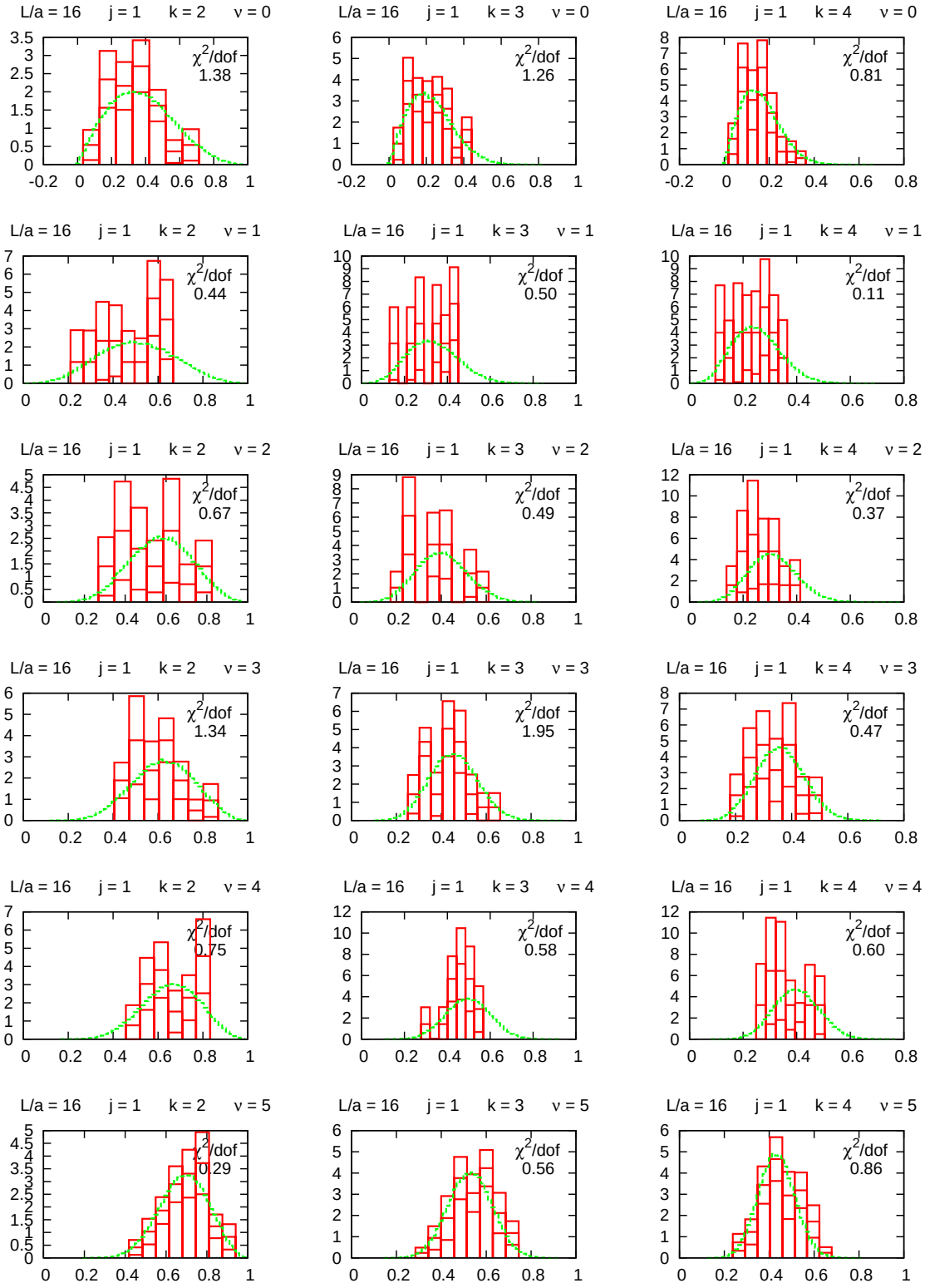

Figure 5: Distribution of the ratios λ_j/λ_k in the sectors $\nu = 0, 1, 2, 3, 4, 5$ for the A_3 lattice and sextet representation. The green (finer) histograms are from RMT, the red histograms are from the simulation including jackknife errors.

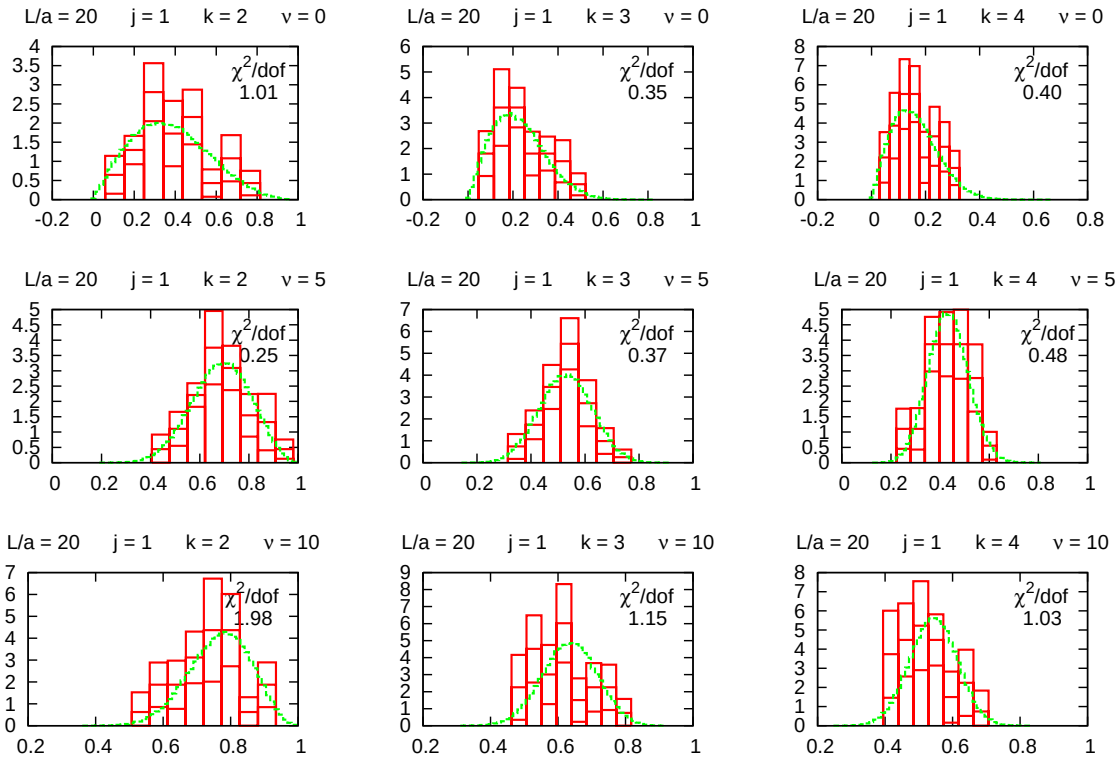

Figure 6: Distribution of the ratios λ_j/λ_k in the sectors $\nu = 0, 5, 10$ for the A_4 lattice and sextet representation. The green (finer) histograms are from RMT, the red histograms are from the simulation including jackknife errors.

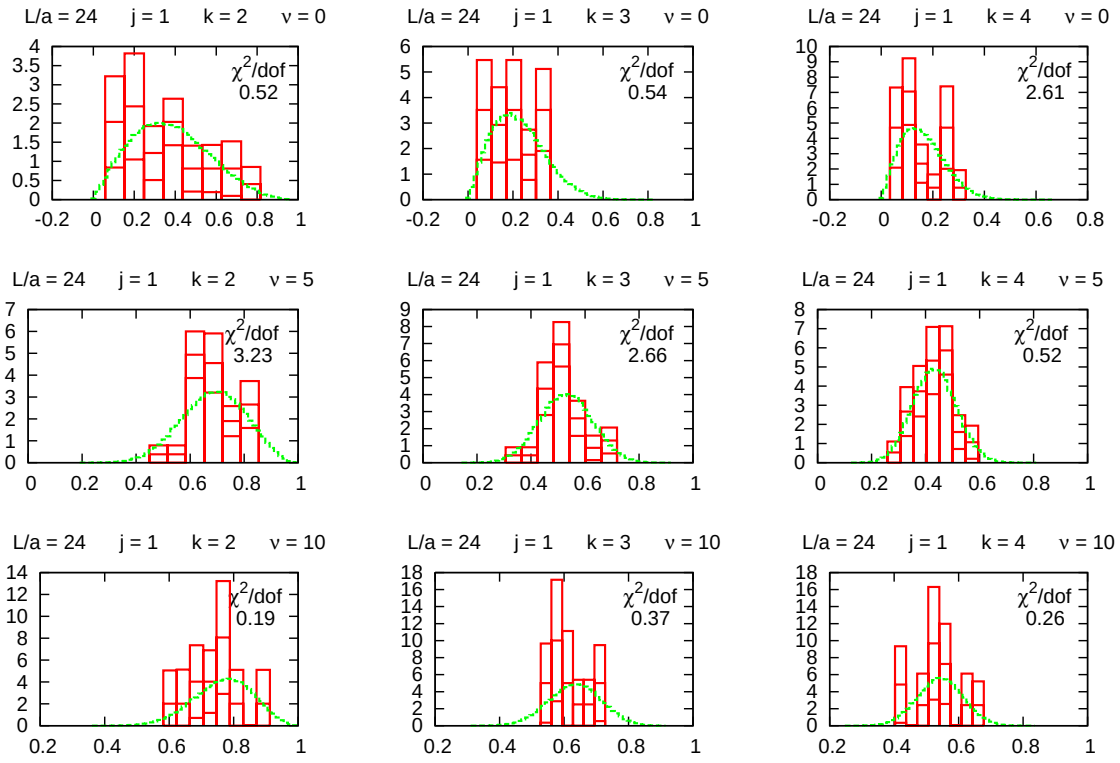

Figure 7: Distribution of the ratios λ_j/λ_k in the sectors $\nu = 0, 5, 10$ for the A_5 lattice and sextet representation. The green (finer) histograms are from RMT, the red histograms are from the simulation including jackknife errors.

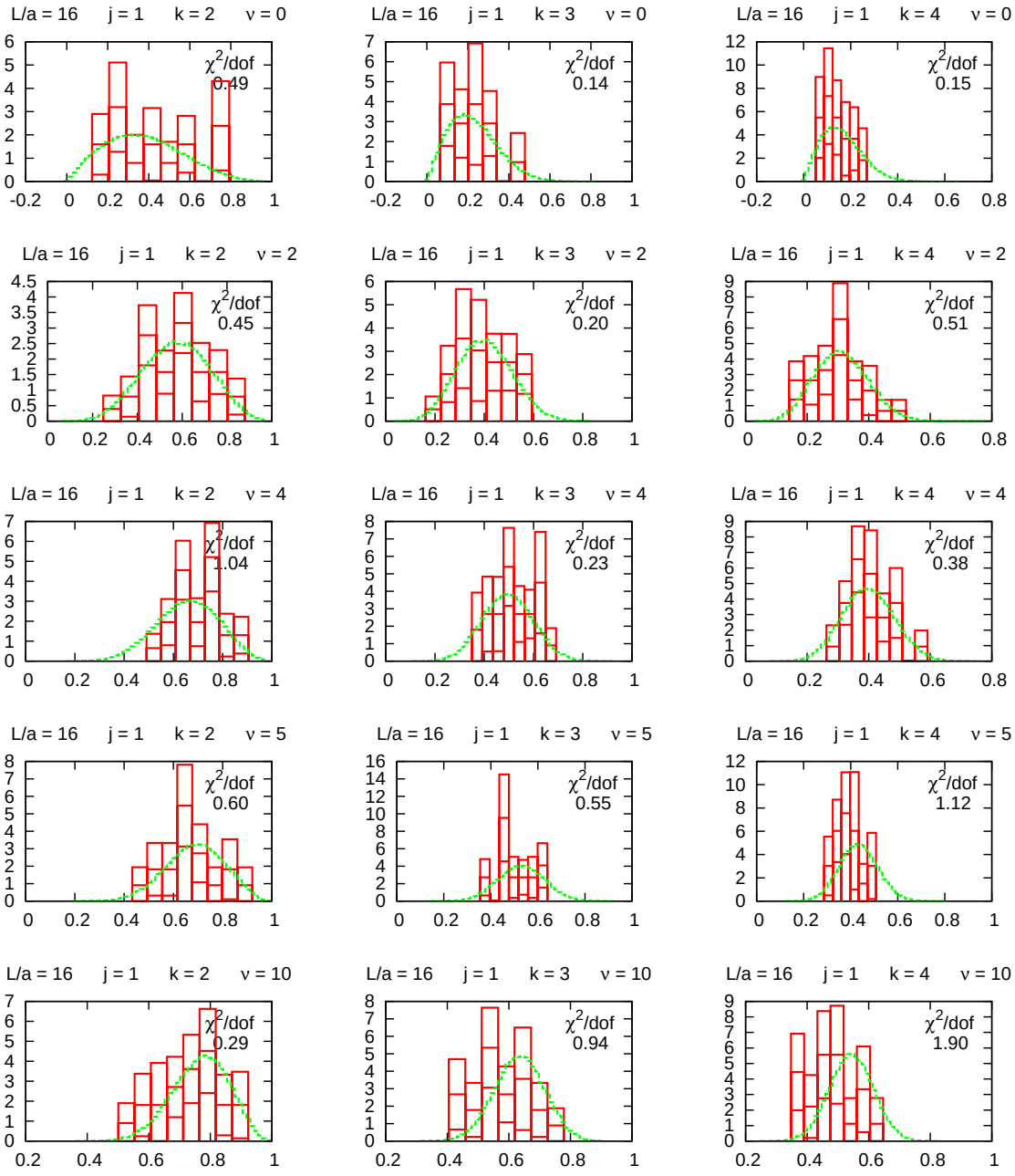

Figure 8: Distribution of the ratios λ_j/λ_k in the sectors $\nu = 0, 2, 4, 5, 10$ for the B_1 lattice and sextet representation. The green (finer) histograms are from RMT, the red histograms are from the simulation including jackknife errors.

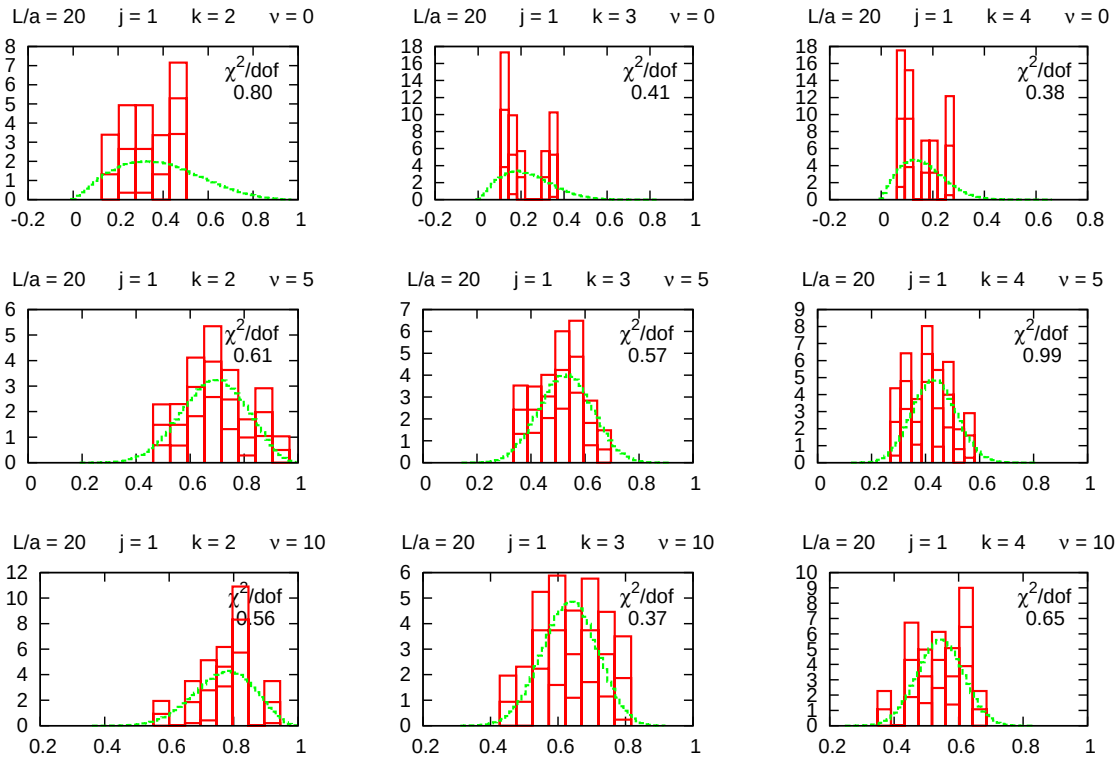

Figure 9: Distribution of the ratios λ_j/λ_k in the sectors $\nu = 0, 5, 10$ for the B_2 lattice and sextet representation. The green (finer) histograms are from RMT, the red histograms are from the simulation including jackknife errors.

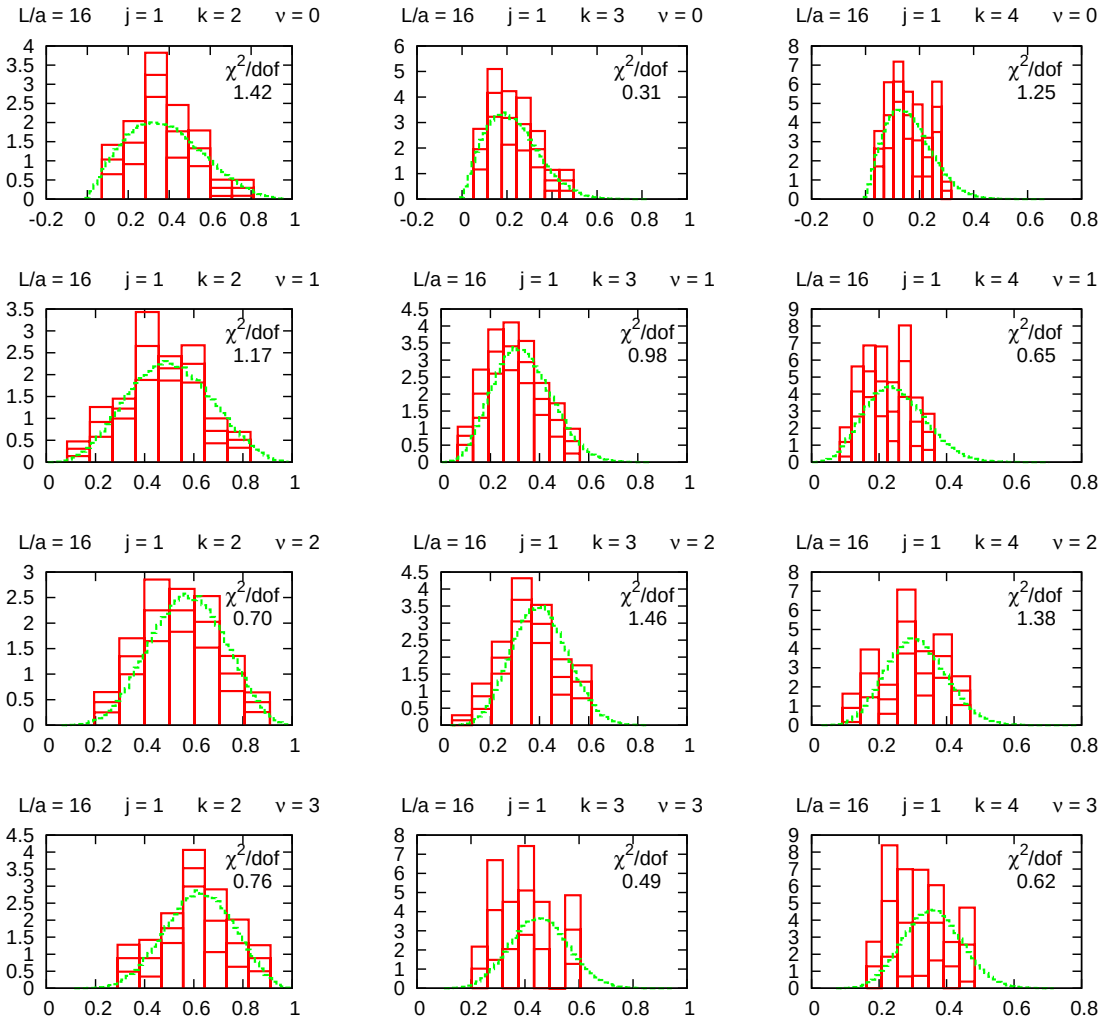

Figure 10: Distribution of the ratios λ_j/λ_k in the sectors $\nu = 0, 1, 2, 3$ for the B_1 lattice and fundamental representation. The green (finer) histograms are from RMT, the red histograms are from the simulation including jackknife errors.

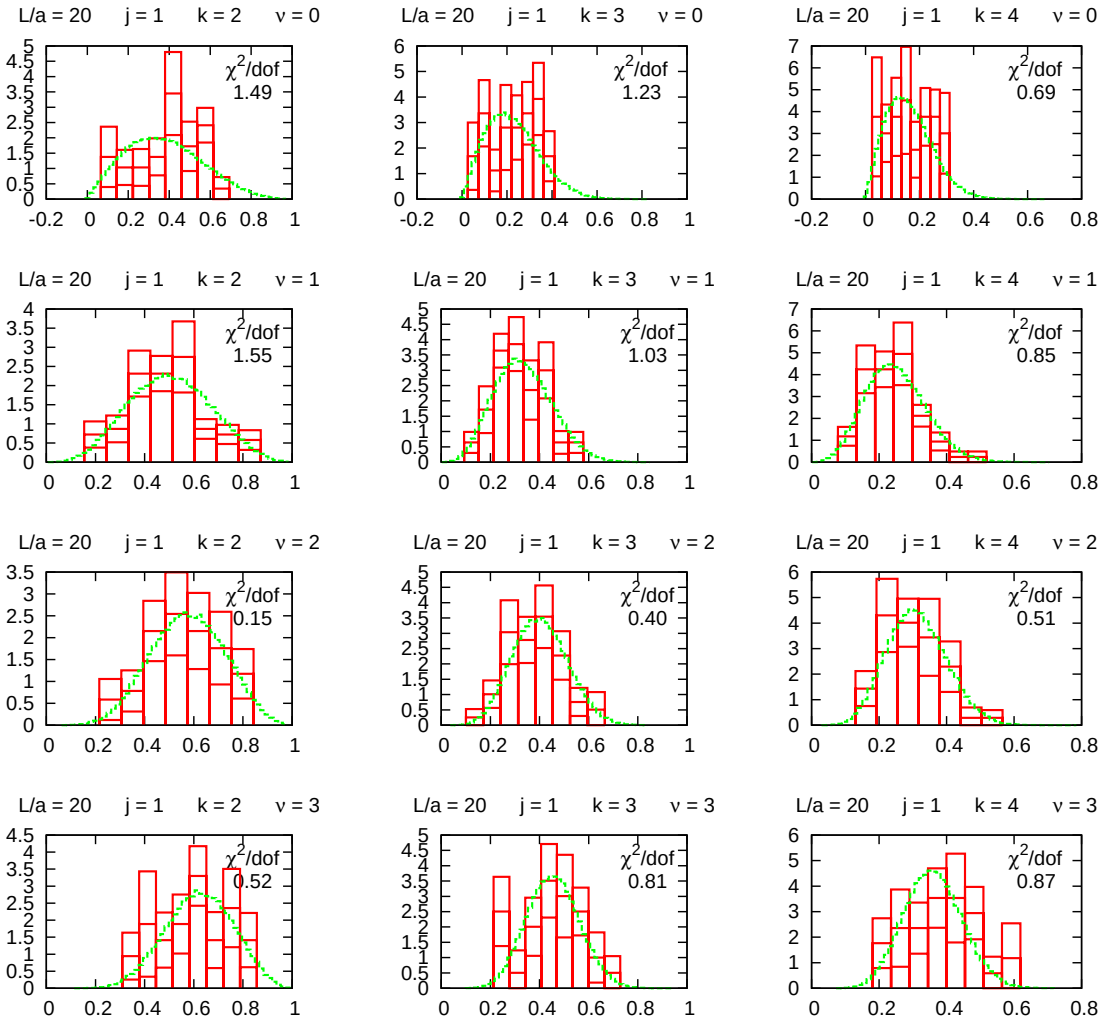

Figure 11: Distribution of the ratios λ_j/λ_k in the sectors $\nu = 0, 1, 2, 3$ for the B_2 lattice and fundamental representation. The green (finer) histograms are from RMT, the red histograms are from the simulation including jackknife errors.